

# Bayesian Constraint Relaxation

Leo L Duan, Alexander L Young, Akihiko Nishimura, David B Dunson

Prior information often takes the form of parameter constraints. Bayesian methods include such information through prior distributions having constrained support. By using posterior sampling algorithms, one can quantify uncertainty without relying on asymptotic approximations. However, *sharply* constrained priors are (a) unrealistic in many settings; and (b) tend to limit modeling scope to a narrow set of distributions that are tractable computationally. We propose to solve both of these problems via a general class of Bayesian *constraint relaxation* methods. The key idea is to replace the sharp indicator function of the constraint holding with an exponential kernel. This kernel decays with distance from the constrained space at a rate depending on a relaxation hyperparameter. By avoiding the sharp constraint, we enable use of off-the-shelf posterior sampling algorithms, such as Hamiltonian Monte Carlo, facilitating automatic computation in broad models. We study the constrained and relaxed distributions under multiple settings, and theoretically quantify their differences. We illustrate the method through multiple novel modeling examples.

KEY WORDS: Constrained Bayes, Constraint functions, Factor models; Manifold constraint, Ordered simplex, Orthonormal; Parameter restrictions; Shrinkage

# 1 Introduction

It is extremely common to have prior information available on parameter constraints in statistical models. For example, one may have prior knowledge that a vector of parameters lies on the probability simplex or satisfies a particular set of inequality constraints. Other common examples include shape constraints on functions, positive semi-definiteness of matrices and orthogonality. There is a very rich literature on optimization subject to parameter constraints. A common approach relies on Lagrange and Karush-Kuhn-Tucker multipliers (Boyd and Vandenberghe, 2004). However, simply producing a point estimate is often insufficient, as uncertainty quantification (UQ) is a key component of most statistical analyses. Usual large sample asymptotic theory, for example showing asymptotic normality of statistical estimators, tends to break down in constrained inference problems. Instead, limiting distributions may have a complex form that needs to be re-derived for each new type of constraint and may be intractable.

An appealing alternative is to rely on Bayesian methods for UQ, including the constraint through a prior distribution having restricted support, and then applying Markov chain Monte Carlo (MCMC) to avoid the need for large sample approximations (Gelfand et al., 1992). Although this strategy appears conceptually simple, there are two clear limitations in practice. First, it is often too restrictive to assume that the parameter exactly satisfies the constraint, and one may want to allow slight deviations. Second, it is in general very difficult to develop tractable posterior sampling algorithms except in special cases. For example, one may be forced to focus on particular forms for the prior and likelihood function to gain tractability and/or may need to develop specially tailored algorithms on a case-by-case basis.

To overcome the first problem, one can attempt to tune the parameters in an un-

constrained prior to place high probability close to the constrained space. However, this approach is limited in scope and often cannot be used. An alternative strategy is to partially enforce the constraint. For example, in considering monotone function estimation, one may impose monotonicity only at a subset of points. However, it is typically difficult to decide exactly which constraints to remove, and outside of specialized cases, this strategy is not appropriate. Hence, to our knowledge, there is essentially no solution to the general problem of how to choose a prior that is concentrated *close* to a particular constrained space.

There is a richer literature on the second problem - posterior sampling under constraints. A common strategy is to reparameterize to reduce the number of constraints and/or simplify the constraints. Examples include reparameterizations of positive semidefinite covariance matrices, probability vectors on the simplex, and spherical parameters. Unfortunately, convenient reparameterizations often are not available and/or may lead to challenges in prior elicitation. A simple and intuitive prior in the original parameterization may induce a complex prior in the new parameterization, motivating the use of *black-box* convenience priors that may conflict with prior knowledge. There are several alternatives focused on particular models for particular constraints. These include both specialized distributions on specific manifolds (e.g., von Mises-Fisher and extensions (Khatri and Mardia, 1977; Hoff, 2009)) and projection-based approaches (Lin and Dunson, 2014). There is also a recent literature developing algorithms for certain classes of manifolds; for example Byrne and Girolami (2013) develop a geodesic Monte Carlo algorithm.

The primary contribution of this article is to propose a broad class of Bayesian priors that are formally close to a constrained space and can effectively solve both of our problems simultaneously. The proposed class is very broad and acts to modify an initial unconstrained prior, having an arbitrary form, to be concentrated near the constrained

space to an extent controlled by a hyperparameter. In addition, due to the simple form and lack of any sharp parameter constraints, general off-the-shelf sampling algorithms can be applied directly. Bypassing the need to develop or code complex and specialized algorithms is a major practical advantage.

The remainder of this article is organized as follows. Section 2 presents the framework for constructing the new class of Bayesian priors, introduces relevant notation, and supplies a general approach for constructing relaxed posteriors when the constrained spaces have positive and zero measure. Representative examples are included. Section 3 contains a discussion of theoretical aspects of our new class of relaxed posteriors, focusing on relationships with sharply constrained posteriors. Section 4 describes how existing classes of efficient posterior sampling algorithms can be applied in our context. Sections 5 and 6 include detailed examples of new modeling attainable through our framework.

## 2 Constraint Relaxation Methodology

### 2.1 Notation and Framework

Assume that  $\theta \in \mathcal{D} \subset \mathcal{R}$  is an unknown continuous parameter, with  $\dim(\mathcal{R}) = r < \infty$ . The constrained sample space  $\mathcal{D}$  is embedded in the  $r$ -dimensional Euclidean space  $\mathcal{R}$ , and can have either zero or positive Lebesgue measure on  $\mathcal{R}$ . The traditional Bayesian approach to including constraints requires a prior density  $\pi_{\mathcal{D}}(\theta)$  with support on  $\mathcal{D}$ . The posterior density of  $\theta$  given data  $Y$  and  $\theta \in \mathcal{D}$  is then

$$\pi_{\mathcal{D}}(\theta | Y) \propto \pi_{\mathcal{D}}(\theta) \mathcal{L}(\theta; Y), \quad (1)$$

where  $\mathcal{L}(\theta; Y)$  is the likelihood function. We assume in the sequel that the restricted prior  $\pi_{\mathcal{D}}(\theta) \propto \pi_{\mathcal{R}}(\theta) \mathbb{1}_{\mathcal{D}}(\theta)$ , with  $\pi_{\mathcal{R}}(\theta)$  an unconstrained distribution on  $\mathcal{R}$  and  $\mathbb{1}_{\mathcal{D}}(\theta)$  an

indicator function that the constraint is satisfied.

As noted in Section 1, there are two primary problems motivating this article. The first is that it is often too restrictive to assume that  $\theta$  is *exactly* within  $\mathcal{D}$  *a priori*, and often is more plausible to assume that  $\theta$  has high probability of falling within a small neighborhood of  $\mathcal{D}$ . The second is that the difficulty of posterior sampling from (1) has greatly limited the scope of modeling, and there is a critical need for general algorithms that are tractable for a broad variety of choices of prior, likelihood and constraint.

In attempting to address these problems, we propose to replace (1) with the following *CO*nstraint *RE*laxed (CORE) posterior density:

$$\tilde{\pi}_\lambda(\theta) \propto \mathcal{L}(\theta; Y) \pi_{\mathcal{R}}(\theta) \exp\left(-\frac{1}{\lambda} \|\nu_{\mathcal{D}}(\theta)\|\right), \quad (2)$$

where we repress the conditioning on data  $Y$  in  $\tilde{\pi}_\lambda(\theta)$  for concise notation and use  $\|\nu_{\mathcal{D}}(\theta)\|$  as a ‘distance’ from  $\theta$  to the constrained space. We assume  $\pi_{\mathcal{R}}(\theta)$  is proper and absolutely continuous with respect to Lebesgue measure  $\mu_{\mathcal{R}}$  on  $\mathcal{R}$ . As such, the constraint relaxed posterior  $\tilde{\pi}_\lambda(\theta)$  corresponds to a coherent Bayesian probability model.

The hyperparameter  $\lambda > 0$  controls how concentrated the prior is around  $\mathcal{D}$ , and as  $\lambda \rightarrow 0$  the kernel  $\exp(-\lambda^{-1} \|\nu_{\mathcal{D}}(\theta)\|)$  converges to  $\mathbb{1}_{\mathcal{D}}(\theta)$  in a pointwise manner. For all  $\lambda > 0$ ,  $\tilde{\pi}_\lambda(\theta)$  introduces support outside of  $\mathcal{D}$ , creating a relaxation of the constraint. Both the value of  $\lambda$  and the choice of  $\|\nu_{\mathcal{D}}(\theta)\|$  are important in controlling the concentration of the prior around  $\mathcal{D}$ . In the next subsection, we discuss the choice of distance. In the subsequent subsections, we discuss details specific to the cases in which  $\mathcal{D}$  has positive and zero measure, respectively.

## 2.2 Distance to Constrained Space

In choosing  $\|\nu_{\mathcal{D}}(\theta)\|$ , a minimal condition is that  $\|\nu_{\mathcal{D}}(\theta)\|$  is zero for  $\theta \in \mathcal{D}$  and positive for  $\theta \notin \mathcal{D}$ . In addition, it is typically appealing for  $\|\nu_{\mathcal{D}}(\theta)\|$  to be increasing as  $\theta$  moves ‘further away’ from the restricted region  $\mathcal{D}$ . It then remains to characterize how we quantify ‘further away’. In this regard, we focus on two types of distances - (I) *Direct Distances* that measure how far  $\theta$  is from  $\mathcal{D}$ ; and (II) *Indirect Distances* that measure how far certain functions of  $\theta$  are from their constrained values when  $\theta \in \mathcal{D}$ .

(I) *Direct Distances*: Let  $\|\nu_{\mathcal{D}}(\theta)\|$  correspond to the distance from  $\theta$  to the closest location in  $\mathcal{D}$ . We focus in particular on the simple choice:

$$\|\nu_{\mathcal{D}}(\theta)\| = \inf_{x \in \mathcal{D}} \|\theta - x\|_k, \quad (3)$$

where  $\|\cdot\|_k$  denotes a  $k$ -norm distance, typically  $k = 1$  or  $2$ .

(II) *Indirect Distances*: Let  $\|\nu_{\mathcal{D}}(\theta)\|$  correspond to

$$\|\nu_{\mathcal{D}}(\theta)\| = \inf_{x \in \mathcal{D}} \|f(\theta) - f(x)\|_k, \quad (4)$$

which reduces to (3) when  $f(\theta) = \theta$ . For example, the constraint may correspond to an upper bound on the function  $f(\theta)$ , so that it is natural to choose  $\|\nu_{\mathcal{D}}(\theta)\|$  to correspond to how far  $f(\theta)$  exceeds this upper bound.

To obtain insight into how the prior concentrates around  $\mathcal{D}$ , and the impact of the choice of distance, it is useful to introduce the concept of  $d$ -expansion of  $\mathcal{D}$ . In particular, the  $d$ -expansion of  $\mathcal{D}$  with respect to  $\|\nu_{\mathcal{D}}(\theta)\|$  is denoted as

$$\mathcal{D}_{\|\nu_{\mathcal{D}}(\theta)\|}(d) = \{\theta \in \mathcal{R} : \|\nu_{\mathcal{D}}(\theta)\| \leq d\},$$

which expands the restricted region  $\mathcal{D}$  to add a ‘halo’ of size  $d$  of  $\theta$  values that are within  $d$  of  $\mathcal{D}$ . Modifying the choice of distance will lead to some changes in the shape of  $\mathcal{D}_{\|\nu_{\mathcal{D}}(\theta)\|}(d)$ .

To illustrate, we consider a constrained space under 3 inequalities  $\mathcal{D} = \{(\theta_1, \theta_2) : \theta_1 > 0, \theta_2 > 0, \theta_1 + \theta_2 < 1\}$ . For type-I distance, we use 2-norm  $\inf_{x \in \mathcal{D}} \|\theta - x\|_2$ . This creates a space expansion of  $\theta$  equally along the boundary  $\partial\mathcal{D}$  (Figure 1(a)). On the other hand, one might be interested in the total violation to the inequalities, as represented in a function  $f(\theta) = (-\theta_1)_+ + (-\theta_2)_+ + (\theta_1 + \theta_2 - 1)_+$  where  $(x)_+ = x$  if  $x > 0$  and 0 otherwise. The associated type-II distance is  $\|\nu_{\mathcal{D}}(\theta)\| = f(\theta)$ , and the expanded neighborhood is shown in Figure 1(b).

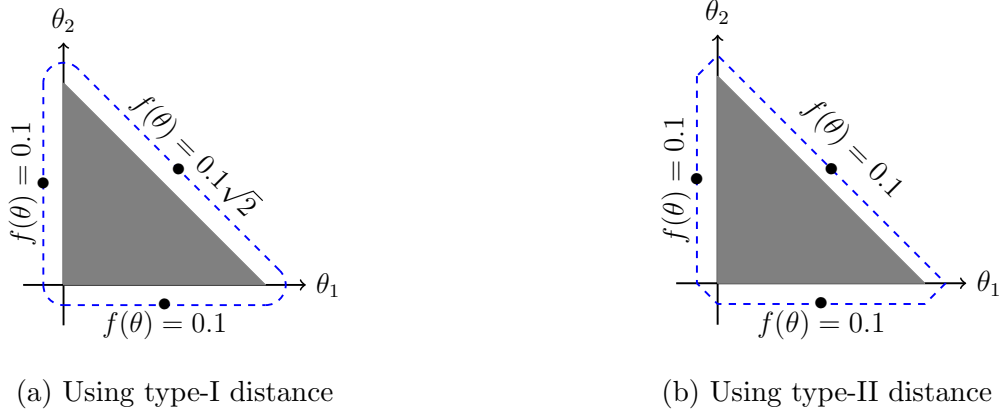


Figure 1: The boundary of the neighborhood (blue dashed line) along  $\|\nu_{\mathcal{D}}(\theta)\| = 0.1$  formed by two types of distances, (a) type-I (direct distance) and (b) type-II (indirect distance), around a constrained space formed by three inequalities (gray area).

The distance can be chosen based on prior belief about how the probability should decrease outside of  $\mathcal{D}$ . In the absence of prior knowledge supporting one choice over another, one can potentially try several different choices, while assessing sensitivity of the results. Even though the precise shape of the  $d$ -expanded regions, and hence the tails of the prior density outside of  $\mathcal{D}$ , can depend on the choice of distance, results are typically essentially indistinguishable practically for different choices. Subtle differences in the  $d$ -expanded

regions, such as those shown in Figure 1, tend to lead to very minimal differences in posterior inferences in our experience.

### 2.3 Constrained Space with Positive Measure

We start with the case when  $\mathcal{D}$  is a subset of  $\mathcal{R}$  with positive Lebesgue measure,  $\mu_{\mathcal{R}}(\mathcal{D}) > 0$ . For technical reasons, we consider only those cases where  $\|\nu_{\mathcal{D}}(\theta)\| > 0$  for  $\mu_{\mathcal{R}}$ -a.e.  $\theta \in \mathcal{R} \setminus \mathcal{D}$ . The sharply constrained density is then simply a truncated version of the unconstrained one, with

$$\pi_{\mathcal{D}}(\theta | Y) = \frac{\mathcal{L}(\theta; Y)\pi_{\mathcal{R}}(\theta)\mathbb{1}_{\mathcal{D}}(\theta)}{\int_{\mathcal{D}}\mathcal{L}(\theta; Y)\pi_{\mathcal{R}}(\theta)d\mu_{\mathcal{R}}(\theta)} \propto \mathcal{L}(\theta; Y)\pi_{\mathcal{R}}(\theta)\mathbb{1}_{\mathcal{D}}(\theta),$$

which is defined with respect to  $\mu_{\mathcal{R}}$ . For constraint relaxation, we replace the indicator with an exponential function of distance

$$\tilde{\pi}_{\lambda}(\theta) = \frac{\mathcal{L}(\theta; Y)\pi_{\mathcal{R}}(\theta)\exp(-\lambda^{-1}\|\nu_{\mathcal{D}}(\theta)\|)}{\int_{\mathcal{R}}\mathcal{L}(\theta; Y)\pi_{\mathcal{R}}(\theta)\exp(-\lambda^{-1}\|\nu_{\mathcal{D}}(\theta)\|)d\mu_{\mathcal{R}}(\theta)} \propto \mathcal{L}(\theta; Y)\pi_{\mathcal{R}}(\theta)\exp(-\lambda^{-1}\|\nu_{\mathcal{D}}(\theta)\|) \quad (5)$$

which is also absolutely continuous with respect to  $\mu_{\mathcal{R}}$ . Direct distances (Type-I) are often natural choices for  $\|\nu_{\mathcal{D}}(\theta)\|$  in this setting.

Expression (5) replaces the function  $\mathbb{1}_{\mathcal{D}}(\theta)$ , which is equal to one for  $\theta \in \mathcal{D}$  and zero for  $\theta \notin \mathcal{D}$ , with  $\exp(-\lambda^{-1}\|\nu_{\mathcal{D}}(\theta)\|)$ , which is still equal to one for  $\theta \in \mathcal{D}$  but decreases exponentially as  $\theta$  moves away from  $\mathcal{D}$ . The prior is effectively *shrinking*  $\theta$  towards  $\mathcal{D}$ , with the exponential tails reminiscent of the double exponential (Laplace) prior that forms the basis of the widely used Lasso procedure. Potentially, we could allow a greater degree of robustness to the choice of  $\mathcal{D}$  by choosing a heavier tailed function in place of the exponential; for example, using the kernel of a generalized double Pareto or t-density. However, such choices introduce an additional hyperparameter, and we focus on the exponential for simplicity.

Section 3.1 addresses the relationship between the strictly constrained posterior density and the relaxed posterior density, identifying cases where inferences become more similar as  $\lambda \rightarrow 0$ . For now, we consider the following example which illustrates how relaxation of the support can provide more realistic modeling.

**Example: Gaussian with inequality constraints**

As a simple illustrative example, we consider a Gaussian likelihood with inequality constraints on the mean. In particular, let

$$y_i \stackrel{iid}{\sim} \text{No}(\theta, 1), \quad i = 1, \dots, n, \quad \pi_{\mathcal{R}}(\theta) = \text{No}(\theta; 0, 1000).$$

Suppose there is prior knowledge that  $\theta < 1$ . The posterior under a sharply constrained model is

$$\pi_{\mathcal{D}}(\theta | Y) \propto \sigma^{-1} \phi\left(\frac{\theta - \mu}{\sigma}\right) \mathbb{1}_{\theta < 1}, \quad \mu = \frac{\bar{y}n}{1/1000 + n}, \quad \sigma^2 = \frac{1}{1/1000 + n},$$

where  $\phi$  denotes the density of the standard Gaussian. This posterior corresponds to  $\text{No}_{(-\infty, 1)}(\mu, \sigma^2)$ , which is a  $\text{No}(\mu, \sigma^2)$  distribution truncated to the region  $\theta < 1$ .

If  $\theta$  is indeed less than one, incorporation of the constraint has the benefit of reducing uncertainty in the posterior distribution, leading to greater concentration around the true value. However, even slight misspecification of the constrained region can lead to biased inferences; for example, perhaps  $\theta = 1.2$ . In this case, as the sample size  $n$  increases, the sharply constrained posterior distribution  $\text{No}_{(-\infty, 1)}(\mu, \sigma^2)$  becomes more and more concentrated near the  $\theta = 1$  boundary as illustrated in Figure 2(a).

The constraint relaxed (CORE) approach is well justified in this case as it allows some probability to be allocated to the  $\theta > 1$  region under the posterior:

$$\tilde{\pi}_{\lambda}(\theta) \propto \sigma^{-1} \phi\left(\frac{\theta - \mu}{\sigma}\right) \exp\left(-\frac{(\theta - 1)_+}{\lambda}\right), \quad \mu = \frac{\bar{y}n}{1/1000 + n}, \quad \sigma^2 = \frac{1}{1/1000 + n}$$

where  $(\theta - 1)_+$  is the direct distance to the constrained space. With a small value  $\lambda = 10^{-2}$ , representing high prior concentration very close to  $\mathcal{D} = (-\infty, 1)$ , the relaxed posterior is close to the sharply constrained one for small to moderate sample sizes, as illustrated in Figure 2(b). However, as  $n$  increases, the posterior becomes concentrated around the true  $\theta$  value, even when it falls outside of the constrained space.

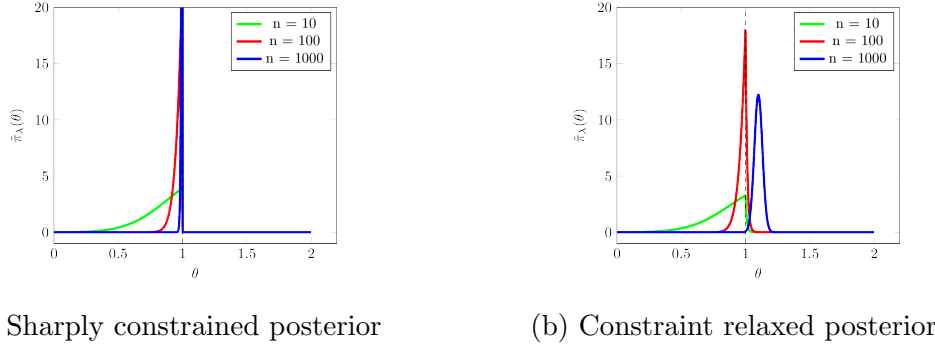


Figure 2: Posterior densities for a Gaussian mean ( $\theta$ ) under sharp (panel (a)) and relaxed constraints (panel (b)). The constraint region is  $\mathcal{D} = (-\infty, 1)$  and the true value is  $\theta = 1.2$ , which falls slightly outside  $\mathcal{D}$  representing misspecification.

## 2.4 Constrained Space with Zero Measure

We now consider the case in which  $\mathcal{D}$  is a measure zero subset of  $\mathcal{R}$  with respect to  $\mu_{\mathcal{R}}$ , the Lebesgue measure on  $\mathcal{R}$ . Since  $\mathcal{D}$  is measure zero, the sharply constrained posterior density can no longer be constructed by truncating the unconstrained posterior on  $\mathcal{D}$  and renormalizing. Rather, one must first use techniques from geometric measure theory to define a regular conditional probability for sharp constraints on  $\mathcal{D}$ . This additional step gives rise to a number of technical difficulties, discussed in more detail in Section 3. Most notably, the use of regular conditional probability alters the formulation of the distance

function  $\|\nu_{\mathcal{D}}(\theta)\|$  used in constraint relaxation.

As a motivating example, suppose the constrained space is the line  $\mathcal{D} = \{\theta : \theta_1 + \theta_2 = 1\}$  and  $\pi_{\mathcal{R}}(\theta) = 1\{\theta_1 \in (0, 1), \theta_2 \in (0, 1)\}$  is a uniform distribution on the unit square. As  $\mu_{\mathcal{R}}(\mathcal{D}) = 0$ , the sharply constrained posterior (5) is undefined. To circumvent this issue, one possibility is to replace  $(\theta_1, \theta_2)$  with  $(\theta_1, 1 - \theta_1)$ , reducing the dimension of the problem. This approach is equivalent to building a regular conditional probability on  $\mathcal{D}$  (see Section 3.2) which results in a posterior density defined with respect to the normalized 1-Hausdorff measure (arclength) on  $\mathcal{D}$ . However, in this reparameterized lower dimensional setting, the constraint is strictly enforced, eliminating any relaxation away from  $\mathcal{D}$ .

Alternatively, one can create a relaxed posterior in the following manner. Motivated by the original constraint,  $\theta_1 + \theta_2 = 1$ , we set  $\nu_{\mathcal{D}}(\theta) = \theta_1 + \theta_2 - 1$  so that  $\|\nu_{\mathcal{D}}(\theta)\| = 0$  when  $\theta \in \mathcal{D}$  and is positive otherwise. With this distance function, we define the relaxed posterior as

$$\begin{aligned}\tilde{\pi}_{\lambda}(\theta) &\propto \mathcal{L}(\theta; Y)\pi_{\mathcal{R}}(\theta) \exp\left(-\frac{\|\nu_{\mathcal{D}}(\theta)\|}{\lambda}\right) \\ &= \mathcal{L}(\theta; Y) \exp\left(-\frac{\|\theta_1 + \theta_2 - 1\|}{\lambda}\right) \mathbb{1}\{(\theta_1 \in (0, 1), \theta_2 \in (0, 1))\}.\end{aligned}$$

This density, defined with respect to Lebesgue measure on the plane, makes use of the original constraint,  $\theta_1 + \theta_2 = 1$ , to define a distance function which in turn allows for relaxation away from the constrained space.

In the preceding example, the constrained space was defined in terms of an equation involving the components of the parameter  $\theta$ . Many other constraints, such as simplex or Stiefel manifold constraints, can be expressed similarly. Thus, it is natural to restrict ourselves to the setting in which  $\mathcal{D}$  can be represented implicitly as the unique solution set of a consistent system of equations  $\{\nu_j(\theta) = 0\}_{j=1}^s$ . The constraint functions,  $\{\nu_j\}_{j=1}^s$ , must satisfy additional assumptions as stated in Section 3.2. For the moment, we highlight their

use in defining a distance to the constrained space and constructing the sharply constrained posterior.

Given a set of constraint functions, let  $\nu_{\mathcal{D}}(\theta) = [\nu_1(\theta), \dots, \nu_s(\theta)]^T$  be a vector valued function from  $\mathcal{R}$  to the  $s$ -dimensional Euclidean space  $\mathbb{R}^s$ . Note that  $\nu_{\mathcal{D}}$  need not be onto  $\mathbb{R}^s$ . Throughout this subsection, we then define the distance function as  $\|\nu_{\mathcal{D}}(\theta)\| = \|\nu_{\mathcal{D}}(\theta)\|_1 = \sum_{j=1}^s |\nu_j(\theta)|$ . The terms  $|\nu_j(\theta)|$  typically take the form of type-II distances as discussed in Section 2.1. Under some mild assumptions on the constraint functions, the preimages,  $\nu_{\mathcal{D}}^{(-1)}(x)$ , will be  $(r-s)$ -dimensional submanifolds of  $\mathcal{R}$  for  $\mu_{\mathbb{R}^s}$ -almost every  $x$  in the range of  $\nu_{\mathcal{D}}$ . In particular,  $\nu_{\mathcal{D}}^{(-1)}(0) = \mathcal{D}$ . Observe that in the motivating example, the pre-images  $\nu_{\mathcal{D}}^{(-1)}(x)$  are the lines  $\theta_1 + \theta_2 = x + 1$  which are also one-dimensional sub-manifolds of  $\mathcal{R}$  similar to  $\mathcal{D}$ .

More generally, while  $\mathcal{D}$  has zero  $r$ -dimensional Lebesgue measure, corresponding to zero volume within  $\mathcal{R}$ , it will have non-zero  $(r-s)$ -dimensional surface area, corresponding to the normalized  $(r-s)$ -dimensional Hausdorff measure, denoted by  $\bar{\mathcal{H}}^{(r-s)}$ . To construct the sharply constrained posterior density, we renormalize the fully constrained density by its integral with respect to the normalized  $(r-s)$ -dimensional Hausdorff measure yielding a valid probability on the constrained space also known as a regular conditional probability. Using the normalized Hausdorff measure, we take

$$\pi_{\mathcal{D}}(\theta | Y) = \frac{\mathcal{L}(\theta; Y)\pi_{\mathcal{R}}(\theta)J^{-1}(\nu_{\mathcal{D}}(\theta))\mathbb{1}_{\mathcal{D}}(\theta)}{\int_{\mathcal{D}} \mathcal{L}(\theta; Y)\pi_{\mathcal{R}}(\theta)J^{-1}(\nu_{\mathcal{D}}(\theta))d\bar{\mathcal{H}}^{(r-s)}(\theta)} \propto \mathcal{L}(\theta; Y)\pi_{\mathcal{R}}(\theta)J^{-1}(\nu_{\mathcal{D}}(\theta))\mathbb{1}_{\mathcal{D}}(\theta),$$

where the Jacobian of  $\nu_{\mathcal{D}}$ ,  $J(\nu_{\mathcal{D}}(\theta)) = \sqrt{(D\nu_{\mathcal{D}})'(D\nu_{\mathcal{D}})}$ , is assumed to be positive and arises from the co-area formula (Federer, 2014). The Jacobian, in part, accounts for the differences in dimension between  $\mathcal{D}$  and  $\mathcal{R}$ .

As in the positive measure case, to relax the constraint we begin with (1) and replace the indicator function with  $\exp(-\|\nu_{\mathcal{D}}(\theta)\|/\lambda)$ , adding support for  $\|\nu_{\mathcal{D}}(\theta)\| > 0$ . Therefore,

the relaxed density is

$$\tilde{\pi}_\lambda(\theta) \propto \mathcal{L}(\theta; Y)\pi_{\mathcal{R}}(\theta) \exp\left(-\frac{1}{\lambda}\|\nu_{\mathcal{D}}(\theta)\|\right) = \mathcal{L}(\theta; Y)\pi_{\mathcal{R}}(\theta) \exp\left(-\frac{1}{\lambda}\sum_{j=1}^s \|\nu_j(\theta)\|\right). \quad (6)$$

Unlike the sharply constrained density however, the relaxed density is supported on  $\mathcal{R}$  and is defined with respect to  $\mu_{\mathcal{R}}$ . One important result of this difference is that the Jacobian of  $\nu_{\mathcal{D}}$  does not appear in (6). As a result, the sharply constrained posterior density is no longer a pointwise limit of the relaxed density in general. The Supplementary Materials contain an example of constraint relaxed modeling on the torus in  $\mathbb{R}^3$ .

## 3 Theory

In this section, we present theoretic details pertaining to the behavior of the relaxed posterior. The primary focus will be on differences in the posterior expectation,  $\mathbb{E}[g(\theta)]$ , under the sharp versus relaxed posteriors. Theorems bounding these differences in terms of  $\lambda$  are presented for a suitable class of functions. All proofs are in the appendix.

Section 3.1 addresses the case in which  $\mathcal{D}$  has positive measure, while Section 3.2 considers the more challenging measure zero case. Additionally, in Section 3.2, we offer a deeper exposition on the geometric measure theory concepts used in the construction of the constrained posterior, present additional properties required of the constraint functions,  $\{\nu_j\}_{j=1}^s$ , and state suitable choices of constraints for some common examples.

### 3.1 Constrained Space with Positive Measure

We focus on quantifying the difference between the sharply constrained and relaxed posterior distributions, both of which are absolutely continuous with respect to Lebesgue

measure on  $\mathcal{R}$ . The posterior expectation of  $g$  under the sharply constrained prior is

$$\mathbb{E}[g(\theta)|\theta \in \mathcal{D}] = \int_{\mathcal{D}} g(\theta) \pi_{\mathcal{D}}(\theta|Y) d\mu_{\mathcal{R}}(\theta) = \frac{\int_{\mathcal{D}} g(\theta) \mathcal{L}(\theta; Y) \pi_{\mathcal{R}}(\theta) d\mu_{\mathcal{R}}(\theta)}{\int_{\mathcal{D}} \mathcal{L}(\theta; Y) \pi_{\mathcal{R}}(\theta) d\mu_{\mathcal{R}}(\theta)}. \quad (7)$$

Similarly, the posterior expectation of  $g$  under the relaxed prior is

$$\mathbb{E}_{\tilde{\pi}_{\lambda}}[g(\theta)] = \int_{\mathcal{R}} g(\theta) \tilde{\pi}_{\lambda}(\theta) d\mu_{\mathcal{R}}(\theta) = \frac{\int_{\mathcal{R}} g(\theta) \mathcal{L}(\theta; Y) \pi_{\mathcal{R}}(\theta) \exp(-\|\nu_{\mathcal{D}}(\theta)\|/\lambda) d\mu_{\mathcal{R}}(\theta)}{\int_{\mathcal{R}} \mathcal{L}(\theta; Y) \pi_{\mathcal{R}}(\theta) \exp(-\|\nu_{\mathcal{D}}(\theta)\|/\lambda) d\mu_{\mathcal{R}}(\theta)}. \quad (8)$$

A short calculation shows that the magnitude of the difference  $\mathbb{E}[g(\theta)|\theta \in \mathcal{D}] - \mathbb{E}_{\tilde{\pi}_{\lambda}}[g(\theta)]$  depends on two quantities: the posterior probability of  $\mathcal{D}$  under the unconstrained posterior, and the average magnitude of  $|g(\theta)|$  over  $\mathcal{R} \setminus \mathcal{D}$  with respect to the relaxed posterior. These results are summarized in Lemma 1.

**Lemma 1.** *Suppose  $g \in \mathbb{L}^1(\mathcal{R}, \mathcal{L}(\theta; Y) \pi_{\mathcal{R}}(\theta) d\mu_{\mathcal{R}})$ . Then,*

$$\left| \mathbb{E}[g(\theta) | \theta \in \mathcal{D}] - \mathbb{E}_{\tilde{\pi}_{\lambda}}[g(\theta)] \right| \leq \frac{\int_{\mathcal{R} \setminus \mathcal{D}} (C_{\mathcal{R}} \mathbb{E}|g(\theta)| + |g(\theta)|) \mathcal{L}(\theta; Y) \pi_{\mathcal{R}}(\theta) \exp(-\|\nu_{\mathcal{D}}(\theta)\|/\lambda) d\mu_{\mathcal{R}}(\theta)}{\left[ \int_{\mathcal{D}} \mathcal{L}(\theta; Y) \pi_{\mathcal{R}}(\theta) d\mu_{\mathcal{R}}(\theta) \right]^2}$$

where  $\mathbb{E}|g(\theta)| \propto \int_{\mathcal{R}} |g(\theta)| \mathcal{L}(\theta; Y) \pi_{\mathcal{R}}(\theta) d\mu_{\mathcal{R}}(\theta)$  is the expected value of  $|g(\theta)|$  with respect to the unconstrained posterior density and  $C_{\mathcal{R}} = \int_{\mathcal{R}} \mathcal{L}(\theta; Y) \pi_{\mathcal{R}}(\theta) d\mu_{\mathcal{R}}(\theta)$  is the normalizing constant of this unconstrained posterior density. Furthermore, if  $\|\nu_{\mathcal{D}}(\theta)\|$  is zero for all  $\theta \in \mathcal{D}$  and positive for  $\mu_{\mathcal{R}}$ -a.e.  $\theta \in \mathcal{R} \setminus \mathcal{D}$ , it follows from the dominated convergence theorem that

$$\left| \mathbb{E}[g(\theta)|\theta \in \mathcal{D}] - \mathbb{E}_{\tilde{\pi}_{\lambda}}[g(\theta)] \right| \rightarrow 0 \text{ as } \lambda \rightarrow 0^+.$$

While this Lemma indicates  $\mathbb{E}_{\tilde{\pi}_{\lambda}}[g(\theta)] \rightarrow \mathbb{E}[g(\theta)|\theta \in \mathcal{D}]$  as  $\lambda \rightarrow 0^+$ , for a fixed  $\lambda > 0$ , large differences can arise if (i)  $|g(\theta)| \mathcal{L}(\theta; Y) \gg \exp(-\lambda^{-1} \|\nu_{\mathcal{D}}(\theta)\|)$  on average over a subset of  $\mathcal{R} \setminus \mathcal{D}$  or (ii) the posterior probability of  $\mathcal{D}$  is small with respect to the unconstrained posterior.

With regards to (i), consider the case where  $\mathcal{F}$  is a measurable subset of  $\mathcal{R}$  for which  $\mathcal{F} \cap \mathcal{D} = \emptyset$  and let  $g(\theta) = \mathbb{1}_{\mathcal{F}}(\theta)$ . Then,  $\mathbb{E}[g(\theta)|\theta \in \mathcal{D}] = 0$ . However,  $\mathbb{E}_{\tilde{\pi}_\lambda}[g(\theta)]$  may be large if  $\mathcal{L}(\theta; Y) \gg \exp(-\lambda^{-1}\|\nu_{\mathcal{D}}(\theta)\|)$  for  $\theta \in \mathcal{F}$ . As such, over  $\mathcal{F}$  the likelihood is dominating the relaxation allowing the CORE density to assign positive probability to  $\mathcal{F}$  which is not possible for the sharply constrained density.

In the case of (ii), the error is inversely proportional to the square of the unconstrained posterior probability of  $\mathcal{D}$ . Thus, when  $\theta \in \mathcal{D}$  is unlikely under the unconstrained model any relaxation away from the constraint is amplified. This effect in particular demonstrates the usefulness of constraint relaxation. If constraints are misspecified and  $\theta \in \mathcal{D}$  is not supported by the data, the posterior estimates using the relaxed density can display a large sensitivity to the choice of  $\lambda$  indicating that the constraints themselves should be re-evaluated.

Turning to the issue of using CORE to estimate posterior expectation of  $g$  under sharp constraints, Lemma 1 indicates that one can obtain sufficiently accurate estimates of  $\mathbb{E}[g(\theta)|\theta \in \mathcal{D}]$  by sampling from  $\tilde{\pi}_\lambda$  when  $\lambda$  is sufficiently small. From a practical standpoint, it is desirable to understand the rate at which  $\mathbb{E}_{\tilde{\pi}_\lambda}[g(\theta)]$  converges to  $\mathbb{E}[g(\theta)|\theta \in \mathcal{D}]$ . The answer ultimately depends on the choice of distance function and its behavior on  $\mathcal{R} \setminus \mathcal{D}$ . We supply the following theorem when the distance function  $\|\nu_{\mathcal{D}}(\theta)\| = \inf_{x \in \mathcal{D}} \|\theta - x\|_2$ . One can use the analysis contained in the proof of this theorem (Appendix A) as a guide to construct convergence rates for a different choice of  $\|\nu_{\mathcal{D}}(\theta)\|$ .

**Theorem 1.** *In addition to the assumptions of Lemma 1, suppose  $g \in \mathbb{L}^2(\mathcal{R}, \mathcal{L}(\theta; Y)\pi_{\mathcal{R}}(\theta)d\mu_{\mathcal{R}})$ ,  $\|\nu_{\mathcal{D}}(\theta)\| = \inf_{x \in \mathcal{D}} \|\theta - x\|_2$ ,  $\mathcal{D}$  has a piecewise smooth boundary, and that  $\mathcal{L}(\theta; Y)\pi_{\mathcal{R}}(\theta)$  is continuous on an open neighborhood containing  $\mathcal{D}$ . Then for  $0 < \lambda \ll 1$ ,*

$$|\mathbb{E}[g(\theta)|\theta \in \mathcal{D}] - \mathbb{E}_{\tilde{\pi}_\lambda}[g(\theta)]| = O(\sqrt{\lambda}).$$

This theorem follows by applying the Cauchy-Schwartz inequality to the term in the numerator of the bound given in Lemma 1. This bound holds for general, even unbounded  $\mathcal{D}$ . More details regarding the coefficient in the error rate are contained in the proof but omitted here for brevity.

### 3.2 Constrained Space with Zero Measure

We begin with a review of some important concepts of geometric measure theory. In addition to supporting the analysis, we are reviewing these topics to offer insight into the behavior of the relaxed posterior. We begin with the definition of the  $d$ -dimensional Hausdorff measure.

**Definition - Hausdorff Measure.** *Let  $A \subset \mathbb{R}^r$ . Fix  $d \leq r$ . Then*

$$\mathcal{H}^d(A) = \liminf_{\delta \rightarrow 0} \left\{ \sum [diam(S_i)]^d : A \subseteq \bigcup S_i, diam(S_i) \leq \delta, diam(S_i) = \sup_{x,y \in S} \|x - y\| \right\}.$$

We denote the normalized  $d$ -dimensional Hausdorff measure as  $\bar{\mathcal{H}}^d(A) = \frac{\Gamma(\frac{1}{2})^d}{2^d \Gamma(\frac{d}{2} + 1)} \mathcal{H}^d(A)$ . When  $d = r$ , Lebesgue and normalized Hausdorff measures coincide  $\mu_{\mathbb{R}^m}(A) = \bar{\mathcal{H}}^d(A)$  (Evans and Gariepy, 2015). Additionally, for a subset  $\mathcal{D}$ , there exists a unique, critical value  $d$  such that  $\bar{\mathcal{H}}^s(\mathcal{D}) = 0$  for  $s > d$  and  $\infty$  for  $s < d$ . The critical value,  $d$ , is referred to as the Hausdorff dimension of  $\mathcal{D}$ , which agrees with the usual notion of dimension when  $\mathcal{D}$  is a piecewise smooth manifold. In fact, when  $\mathcal{D}$  is a compact,  $d$ -dimensional submanifold of  $\mathbb{R}^m$ , it will have Hausdorff dimension  $d$  so that  $\bar{\mathcal{H}}^d(\mathcal{D})$  is the  $d$ -dimensional surface area of  $A$ . In the zero measure setting, as discussed in Section 2, we are focusing on the case where  $\mathcal{D}$  is an  $(r - s)$ -dimensional submanifold of  $\mathcal{R}$ . As such, it is natural to define the sharply constrained posterior with respect to  $\bar{\mathcal{H}}^{r-s}$ , which is referred to as a regular conditional probability or *r.c.p* (Diaconis et al. (2013)).

Defining the r.c.p on the measure zero constrained space  $\mathcal{D}$  and the subsequent analysis requires the co-area formula.

**Theorem 2.** *Co-area formula (Diaconis et al., 2013; Federer, 2014) Suppose  $v : \mathbb{R}^r \rightarrow \mathbb{R}^s$ , with  $s < r$ , is Lipschitz and that  $g \in \mathbb{L}^1(\mathbb{R}^r, \mu_{\mathbb{R}^r})$ . Assume  $J[v(\theta)] > 0$ , then*

$$\int_{\mathbb{R}^r} g(\theta) J[v(\theta)] d\mu_{\mathbb{R}^r}(\theta) = \int_{\mathbb{R}^s} \left( \int_{v^{-1}(y)} g(\theta) d\bar{\mathcal{H}}^{r-s}(\theta) \right) d\mu_{\mathbb{R}^s}(y). \quad (9)$$

Recall, we previously assumed that  $\mathcal{D}$  can be defined implicitly as the solution set to a system of  $s$  equations,  $\{\nu_j(\theta) = 0\}_{j=1}^s$ , and we defined the map  $\nu_{\mathcal{D}}(\theta) = [\nu_1(\theta), \dots, \nu_s(\theta)]$  from our parameter space,  $\mathcal{R}$ , to the Euclidean space,  $\mathbb{R}^s$ . These constraint functions must adhere to some additional restrictions.

- (a)  $\nu_j : \mathcal{R} \rightarrow \mathbb{R}$  is Lipschitz continuous,
- (b)  $\nu_j(\theta) = 0$  only for  $\theta \in \mathcal{D}$ ,
- (c) for  $j = 1, \dots, s$ , the pre-image  $\nu_j^{(-1)}(x)$  is a co-dimension 1 sub-manifold of  $\mathcal{R}$  for  $\mu_{\mathbb{R}}$ -a.e.  $x$  in the range of  $\nu_j$ ,
- (d)  $\nu_j^{(-1)}(0)$  and  $\nu_k^{(-1)}(0)$  intersect transversally for  $1 \leq j < k \leq s$ .

Property (a) guarantees that  $\nu_{\mathcal{D}}$  is itself Lipschitz so the co-area formula applies. The remaining properties (b)-(d) are constructed so that when  $x \in \mathbb{R}^s$  is near zero, the preimage  $\nu_{\mathcal{D}}^{(-1)}(x)$  is also an  $(r-s)$ -dimensional submanifold corresponding to a perturbation of the constrained space  $\mathcal{D}$ . In the remainder of this section, we assume that  $\nu_{\mathcal{D}}^{(-1)}(x)$  is an  $(r-s)$ -dimensional submanifold of a.e  $x$  in the range of  $\mathcal{D}$ . While this is a very strong assumption, to attain relaxation near  $\mathcal{D}$ , the transversality condition (d) assures this for  $x$  near 0.

Criteria (a) - (d) may seem restrictive. However, many measure zero constraints can be defined implicitly to satisfy (b) - (d). In Table 1, we offer a few examples. An initial

set of constraint functions can typically be modified to satisfy the Lipschitz condition by truncating the original parameter space  $\mathcal{R}$  or by composing the constraints with bounded functions. The former choice was used for the Unit sphere and Stiefel manifold constraints in the table.

$\mathcal{R}$	$\mathcal{D}$	$\dim(\mathcal{R})$	$\dim(\mathcal{D})$	Constraint functions
$[0, 1]^r$	Probability simplex, $\Delta^{r-1}$	$r$	$r-1$	$\nu_1(\theta) = \sum(\theta) - 1$
$\mathbb{R}^r$	Line, $\text{span}\{\vec{u}\}$ $\vec{u} \neq \vec{0}$	$r$	1	$\nu_j(\vec{\theta}) = \vec{\theta}^T \vec{b}_j$ with $\{\vec{b}_1, \dots, \vec{b}_{r-1}\}$ a basis for $\text{span}\{\vec{u}\}^\perp$
$[-1, 1]^r$	Unit sphere, $\mathbb{S}^{r-1}$	$r$	$r-1$	$\nu_1(\theta) = \ \theta\ ^2 - 1$
$[-1, 1]^{n \times k}$	Stiefel manifold, $\mathcal{V}(n, k)$	$nk$	$nk - \frac{1}{2}k(k+1)$	$\nu_{i,j}(\theta) = \vec{\theta}_i^T \vec{\theta}_j - \delta_{i,j}$ $1 \leq i \leq j \leq k$ and $\delta_{i,j} = \mathbb{1}_{i=j}$

Table 1: Table of constraints for some commonly used constrained spaces.

Given this construction of the constrained space, we can now specify the regular conditional probability of  $\theta$ , given  $\theta \in \mathcal{D}$ .

**Theorem 3.** (Diaconis *et al.*, 2013) *Assume that  $J(\nu_{\mathcal{D}}(\theta)) > 0$  and that for each  $z \in \mathbb{R}^s$  there is a finite non-negative  $p_z$  such that,*

$$m^{p_z}(z) = \int_{\nu_{\mathcal{D}}^{-1}(z)} \frac{\mathcal{L}(\theta; Y)\pi_{\mathcal{R}}(\theta)}{J(\nu_{\mathcal{D}}(\theta))} d\bar{\mathcal{H}}^{p_z}(\theta) \in (0, \infty).$$

Then, for any Borel subset  $F$  of  $\mathcal{R}$ , it follows that

$$P(\theta \in F \mid v(\theta) = z) = \begin{cases} \frac{1}{m^{p_z}(z)} \int_F \frac{\mathcal{L}(\theta; Y)\pi_{\mathcal{R}}(\theta)\mathbb{1}_{\nu_{\mathcal{D}}(\theta)=z}}{J(\nu_{\mathcal{D}}(\theta))} d\bar{\mathcal{H}}^{p_z}(\theta) & m^p(z) \in (0, \infty) \\ \delta(F) & m^p(z) \in \{0, \infty\} \end{cases}$$

is a valid regular conditional probability for  $\theta \in \mathcal{D}$ . Here,  $\delta(F) = 1$  if  $0 \in F$  and 0 otherwise.

By construction,  $\{\theta : \nu_{\mathcal{D}}(\theta) = z\}$  is an  $(r-s)$  dimensional submanifold of  $\mathcal{R}$  for  $\mu_{\mathbb{R}^s}$ -a.e.  $z$  in the range of  $\nu_{\mathcal{D}}$ . As such, it follows that one should take  $p_z = r-s$ . While it is still

possible that  $m^p(z) \in \{0, \infty\}$  for some  $z$ , we need not worry about these cases as they occur on a set of  $\mu_{\mathbb{R}^s}$  measure zero. Most importantly, setting  $z = 0$  allows us to define

$$\pi_{\mathcal{D}}(\theta | \theta \in \mathcal{D}, Y) = \frac{1}{m^{r-s}(0)} \frac{\mathcal{L}(\theta; Y) \pi_{\mathcal{R}}(\theta) \mathbb{1}_{\mathcal{D}}(\theta)}{J(\nu_{\mathcal{D}}(\theta))} \quad (10)$$

as the constrained posterior density as originally stated in Section 2.2.

To understand the effects of constraint relaxation, consider a Borel subset,  $\mathcal{F}$ , of  $\mathcal{R}$ . Under the sharply constrained posterior,

$$\begin{aligned} P(\theta \in \mathcal{F} | Y) &= \int_{\mathcal{F}} \pi_{\mathcal{D}}(\theta | Y) d\bar{\mathcal{H}}^{r-s}(\theta) = \frac{\int_{\mathcal{F}} \mathcal{L}(\theta; Y) \pi_{\mathcal{R}}(\theta) J^{-1}(\nu_{\mathcal{D}}(\theta)) \mathbb{1}_{\mathcal{D}}(\theta) d\bar{\mathcal{H}}^{r-s}(\theta)}{\int_{\mathcal{D}} \mathcal{L}(\theta; Y) \pi_{\mathcal{R}}(\theta) J^{-1}(\nu_{\mathcal{D}}(\theta)) \mathbb{1}_{\mathcal{D}}(\theta) d\bar{\mathcal{H}}^{r-s}(\theta)} \\ &= \frac{\int_{\mathcal{F} \cap \mathcal{D}} \mathcal{L}(\theta; Y) \pi_{\mathcal{R}}(\theta) J^{-1}(\nu_{\mathcal{D}}(\theta)) d\bar{\mathcal{H}}^{r-s}(\theta)}{\int_{\mathcal{D}} \mathcal{L}(\theta; Y) \pi_{\mathcal{R}}(\theta) J^{-1}(\nu_{\mathcal{D}}(\theta)) d\bar{\mathcal{H}}^{r-s}(\theta)}. \end{aligned} \quad (11)$$

Alternatively, under the relaxed posterior,

$$P(\theta \in \mathcal{F} | Y) = \int_{\mathcal{F}} \tilde{\pi}_{\lambda}(\theta) d\mu_{\mathcal{R}}(\theta) = \frac{\int_{\mathcal{F}} \mathcal{L}(\theta; Y) \pi_{\mathcal{R}}(\theta) \exp\left(-\frac{1}{\lambda} \sum_{j=1}^s \|\nu_j(\theta)\|\right) d\mu_{\mathcal{R}}(\theta)}{\int_{\mathcal{R}} \mathcal{L}(\theta; Y) \pi_{\mathcal{R}}(\theta) \exp\left(-\frac{1}{\lambda} \sum_{j=1}^s \|\nu_j(\theta)\|\right) d\mu_{\mathcal{R}}(\theta)} \quad (12)$$

Making use of the behavior of the preimages of  $\nu_{\mathcal{D}}$ , we can reexpress (12) through the co-area formula as

$$P(\theta \in \mathcal{F} | Y) = \frac{\int_{\mathbb{R}^s} \left[ \int_{\mathcal{F} \cap \nu_{\mathcal{D}}^{(-1)}(x)} \mathcal{L}(\theta; Y) \pi_{\mathcal{R}}(\theta) J^{-1}(\nu_{\mathcal{D}}(\theta)) d\bar{\mathcal{H}}^{r-s}(\theta) \right] \exp\left(-\frac{1}{\lambda} \|x\|_1\right) d\mu_{\mathbb{R}^s}(x)}{\int_{\mathbb{R}^s} \left[ \int_{\mathcal{R} \cap \nu_{\mathcal{D}}^{(-1)}(x)} \mathcal{L}(\theta; Y) \pi_{\mathcal{R}}(\theta) J^{-1}(\nu_{\mathcal{D}}(\theta)) d\bar{\mathcal{H}}^{r-s}(\theta) \right] \exp\left(-\frac{1}{\lambda} \|x\|_1\right) d\mu_{\mathbb{R}^s}(x)} \quad (13)$$

Similar to the positive measure case, we can also give statements regarding expectation of  $g(\theta)$  under the constrained and relaxed posterior. The posterior expectation of  $g(\theta)$  under the sharp constraint  $\theta \in \mathcal{D}$  is

$$\mathbb{E}[g(\theta) | \theta \in \mathcal{D}] = \mathbb{E}[g(\theta) | \nu_{\mathcal{D}}(\theta) = 0] = \int_{\mathcal{R}} g(\theta) \pi_{\mathcal{D}}(\theta) d\bar{\mathcal{H}}^{r-s}(\theta).$$

Using the definition of  $\tilde{\pi}_\lambda$  from Section 2.2, the expected value of  $g(\theta)$  with respect to the relaxed density, denoted  $\mathbb{E}_{\tilde{\Pi}}[g(\theta)]$ , is

$$\mathbb{E}_{\tilde{\Pi}}[g(\theta)] = \frac{1}{m_\lambda} \int_{\mathcal{R}} g(\theta) \mathcal{L}(\theta; Y) \pi_{\mathcal{R}}(\theta) \exp\left(-\frac{1}{\lambda} \|\nu_{\mathcal{D}}(\theta)\|_1\right) d\mu_{\mathcal{R}}(\theta) \quad (14)$$

where  $m_\lambda = \int_{\mathcal{R}} \mathcal{L}(\theta; Y) \pi_{\mathcal{R}}(\theta) \exp(-\lambda^{-1} \|\nu_{\mathcal{D}}(\theta)\|_1) d\mu_{\mathcal{R}}(\theta)$ . The remaining results of the section are the following statements regarding the use of  $\mathbb{E}_{\tilde{\Pi}}[g(\theta)]$  to estimate  $\mathbb{E}[g(\theta)|\theta \in \mathcal{D}]$ .

**Theorem 4.** *Let  $m : \mathbb{R}^s \rightarrow \mathbb{R}$  and  $G : \mathbb{R}^s \rightarrow \mathbb{R}$  be defined as follows*

$$\begin{aligned} m(x) &= \int_{\nu_{\mathcal{D}}^{-1}(x)} \frac{\mathcal{L}(\theta; Y) \pi_{\mathcal{R}}(\theta)}{J(\nu_{\mathcal{D}}(\theta))} d\bar{\mathcal{H}}^{r-s}(\theta) \\ G(x) &= \int_{\nu_{\mathcal{D}}^{-1}(x)} g(\theta) \frac{\mathcal{L}(\theta; Y) \pi_{\mathcal{R}}(\theta)}{J(\nu_{\mathcal{D}}(\theta))} d\bar{\mathcal{H}}^{r-s}(\theta). \end{aligned}$$

*Suppose that both  $m$  and  $G$  are continuous on an open interval containing the origin and that*

*$g \in \mathbb{L}^1(\mathcal{R}, \mathcal{L}(\theta; Y) \pi_{\mathcal{R}}(\theta) d\mu_{\mathcal{R}})$ . Then,  $|\mathbb{E}_{\tilde{\Pi}}[g(\theta)] - \mathbb{E}[g(\theta)|\theta \in \mathcal{D}]| \rightarrow 0$  as  $\lambda \rightarrow 0^+$ .*

**Corollary 1.** *In addition to the assumptions of Theorem 4, suppose that both  $m$  and  $G$  are differentiable at 0. Then*

$$|\mathbb{E}_{\tilde{\Pi}}[g] - \mathbb{E}[g(\theta)|\theta \in \mathcal{D}]| = O\left(\frac{\lambda}{|\log \lambda|^s}\right)$$

*as  $\lambda \rightarrow 0^+$ .*

The continuity assumptions of Theorem 4 and differentiability assumptions of Corollary 1 have some important consequences. Recall, the pairwise transversal intersection requirement, (d), assures that  $\nu_{\mathcal{D}}^{(-1)}(x)$  behaves like a small perturbation of  $\mathcal{D}$  when  $x$  is near zero. Therefore, if the unconstrained posterior,  $\mathcal{L}(\theta; Y) \pi_{\mathcal{R}}(\theta)$ , the Jacobian,  $J(\nu_{\mathcal{D}}(\theta))$ , and  $g$  are all continuous on an open neighborhood containing  $\mathcal{D}$ , the continuity assumptions of Theorem 4 will follow.

## 4 Posterior Computation

The constraint relaxed posterior density is supported in  $\mathcal{R}$  and can be directly sampled via off-the-shelf tools, such as slice sampling, adaptive Metropolis-Hastings and Hamiltonian Monte Carlo (HMC). In this section, we focus on HMC as a general algorithm that tends to have good performance in a variety of settings.

In order to sample  $\theta$ , HMC introduces an auxiliary momentum variable  $p \sim \text{No}(0, M)$ . The covariance matrix  $M$  is referred to as a *mass matrix* and is typically chosen to be the identity or adapted to approximate the inverse covariance of  $\theta$ . HMC then samples from the joint target density  $\pi(\theta, p) = \pi(\theta)\pi(p) \propto \exp\{-H(\theta, p)\}$  where, in the case of the posterior under relaxation,  $H(\theta, p) = U(\theta) + K(p)$ , with  $U(\theta) = -\log \pi(\theta)$ ,  $K(p) = p'M^{-1}p/2$ , and  $\pi(\theta)$  the unnormalized density in (5) or (6).

From the current state  $(\theta^{(0)}, p^{(0)})$ , HMC generates a Metropolis-Hastings proposal by simulating Hamiltonian dynamics defined by a differential equation:

$$\begin{aligned} \frac{\partial \theta^{(t)}}{\partial t} &= \frac{\partial H(\theta, p)}{\partial p} = M^{-1}p, \\ \frac{\partial p^{(t)}}{\partial t} &= -\frac{\partial H(\theta, p)}{\partial \theta} = -\frac{\partial U(\theta)}{\partial \theta}. \end{aligned} \tag{15}$$

The exact solution to (15) is typically intractable but a valid Metropolis proposal can be generated by numerically approximating (15) with a reversible and volume-preserving integrator (Neal, 2011). The standard choice is the *leapfrog* integrator which approximates the evolution  $(\theta^{(t)}, p^{(t)}) \rightarrow (\theta^{(t+\epsilon)}, p^{(t+\epsilon)})$  through the following update equations:

$$p \leftarrow p - \frac{\epsilon}{2} \frac{\partial U}{\partial \theta}, \quad \theta \leftarrow \theta + \epsilon M^{-1}p, \quad p \leftarrow p - \frac{\epsilon}{2} \frac{\partial U}{\partial \theta} \tag{16}$$

Taking  $L$  leapfrog steps from the current state  $(\theta^{(0)}, p^{(0)})$  generates a proposal  $(\theta^*, p^*) \approx$

$(\theta^{(L\epsilon)}, p^{(L\epsilon)})$ , which is accepted with the probability

$$1 \wedge \exp(-H(\theta^*, p^*) + H(\theta^{(0)}, p^{(0)}))$$

We refer to this algorithm as CORE-HMC. The computing efficiency of HMC under different degrees of relaxation is discussed in the Supplementary Materials.

## 5 Simulated Examples

CORE enables much greater flexibility for general modeling practice. We illustrate two interesting cases via simulated examples.

### Example: Sphere $t$ Distribution

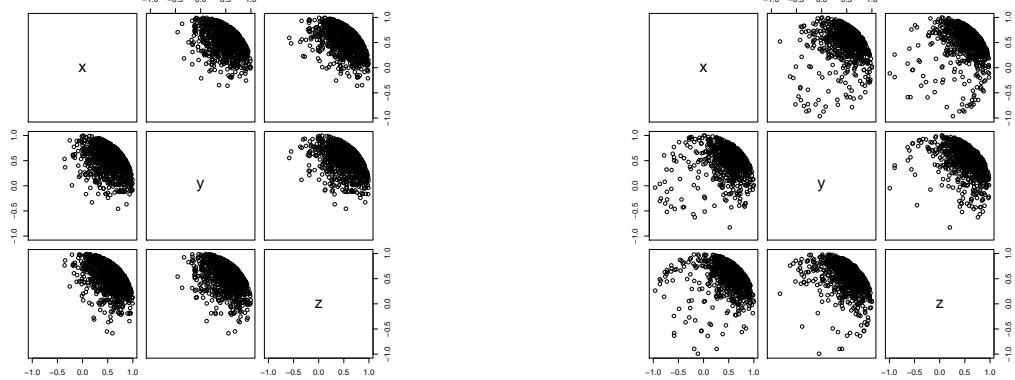
In the first example, we consider modeling on a  $(p-1)$ -sphere  $\mathcal{D} = \mathbb{S}^{p-1}$ . The von Mises–Fisher distribution (Khatri and Mardia, 1977) is the result of constraining a multivariate Gaussian  $\theta \sim \text{No}(F, I\sigma^2)$  with  $F \in \mathcal{D}$  and  $v(\theta) = \theta'\theta - 1$ :

$$\pi_{\mathcal{D}}(\theta) \propto \exp\left(-\frac{\|F - \theta\|^2}{2\sigma^2}\right) \mathbb{1}_{\theta'\theta=1} \propto \exp\left(\frac{F'\theta}{\sigma^2}\right) \mathbb{1}_{\theta'\theta=1}.$$

CORE allows us to easily consider different ‘parent’ unconstrained distributions instead of just the Gaussian. Using  $v(\theta) = \theta'\theta - 1$  to form a distance in CORE, we propose a spherical constraint relaxed  $t$ -density:

$$\tilde{\pi}_{\lambda}(\theta) \propto \left(1 + \frac{\|F - \theta\|^2}{m\sigma^2}\right)^{-\frac{(m+p)}{2}} \exp\left(-\frac{\|\theta'\theta - 1\|}{\lambda}\right),$$

with the parent  $t$ -density having  $m$  degrees of freedom, mean  $F \in \mathcal{D}$  and variance  $I\sigma^2$ . Figure 3 shows that the proposed distribution induces heavier tail behavior than the von Mises–Fisher.



(a) von Mises–Fisher distribution.

(b) Spherical CORE  $t$ -distribution with  $m = 3$ .

Figure 3: Sectional view of random samples from constrained distributions on a unit sphere inside  $\mathbb{R}^3$ . The distributions are derived through conditioning on  $\theta'\theta = 1$  based on unconstrained densities of (a)  $\text{No}(F, \text{diag}\{0.1\})$ , (b)  $t_3(F, \text{diag}\{0.1\})$ , where  $F = [1/\sqrt{3}, 1/\sqrt{3}, 1/\sqrt{3}]'$ . The samples are generated via CORE-HMC with  $\lambda = 10^{-3}$ .

### Example: Ordered Dirichlet Distribution

For the second example, we consider relaxing an ordered Dirichlet distribution, with density:

$$\pi_{\mathcal{D}}(\theta) \propto \prod_{j=1}^J \theta_j^{\alpha_j-1} \mathbb{1}_{\sum_{j=1}^J \theta_j = 1} \prod_{j=1}^{J-1} \mathbb{1}_{\theta_j \geq \theta_{j+1}},$$

where we focus on  $\alpha_j = \alpha$  in our experiments. This ordered Dirichlet distribution produces realizations  $\theta = (\theta_1, \dots, \theta_J)'$  that are on the probability simplex, and restricted to be decreasing  $\theta_1 \geq \theta_2 \geq \dots \geq \theta_J$ .

Dirichlet distributions are routinely used as priors for the probability weights in mixture models. One common problem with such models is non-identifiability between the different components. Ordering the components to have decreasing weight is one way to impose

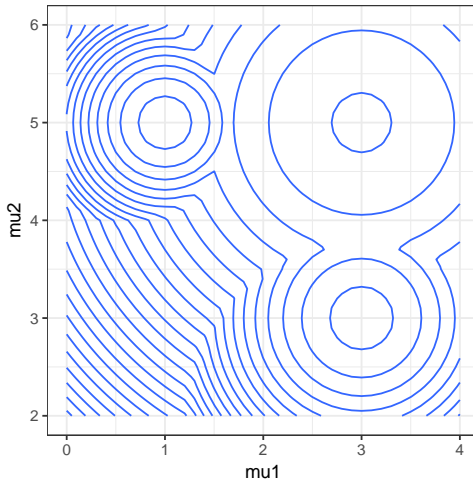
identifiability, but such constraints lead to computational problems. There is a simplex HMC algorithm for posterior sampling under simplex constraints (Betancourt, 2012), but this algorithm can not be used with order restrictions also imposed. Hence, we use CORE to relax the order constraint:

$$\tilde{\pi}_\lambda(\theta) \propto \prod_{j=1}^J \theta_j^{\alpha-1} \mathbb{1}_{\sum_{j=1}^J \theta_j = 1} \prod_{j=1}^{J-1} \exp \left( -\lambda(\theta_{j+1} - \theta_j, 0)_+ \right).$$

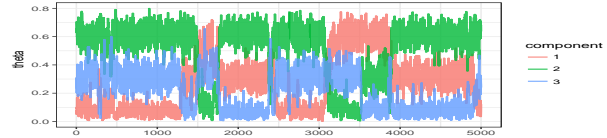
To illustrate the performance, we consider a mixture model for data  $y_i \in \mathbb{R}^2$ , with

$$y_i \sim f, i = 1, \dots, n, \quad f(y) = \sum_{j=1}^3 \theta_j \text{No}(y; \mu_j, \Sigma).$$

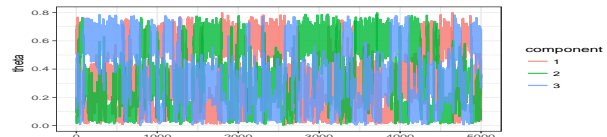
We compare a conventional symmetric Dirichlet prior for  $\theta$  with a constraint relaxed ordered Dirichlet with  $\lambda = 10^{-6}$ . We let  $n = 100$ ,  $\{\theta_1, \theta_2, \theta_3\} = \{0.6, 0.3, 0.1\}$ ,  $\{\mu_1, \mu_2, \mu_3\} = \{[1, 5], [3, 3], [3, 5]\}$  and  $\Sigma = I_2$ . We assign weakly informative priors  $\text{No}(0, 10I_2)$  for each  $\mu_j$  and let  $\Sigma = \text{diag}(\sigma_1^2, \sigma_2^2)$  with  $\sigma_1^2, \sigma_2^2 \sim \text{IG}(2, 1)$ . Figure 4(a) shows contours of the posterior density of  $\mu$ . There is substantial overlap in the different components, leading to label switching in MCMC implementations for the symmetric Dirichlet prior (traceplots in Figure 4(b,c) for Gibbs sampling and HMC), while the ordered Dirichlet with small relaxation shows no label switching (Figure 4(d)).



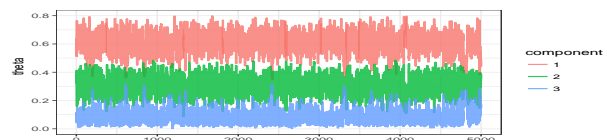
(a) Posterior density of the component means  $\{\mu_j\}_{j=1}^3$ .



(b) Gibbs sampling of unordered Dirichlet



(c) HMC sampling of unordered Dirichlet



(d) HMC sampling of Dirichlet with mildly relaxed order constraint

Figure 4: Contour of the posterior density of mixture component means  $\mu_1, \mu_2, \mu_3$  and traceplot of posterior samples for the component weights  $\theta_1, \theta_2, \theta_3$  in a 3-component normal mixture model. Panel (a) shows that there is significant overlap among component means  $\mu_1, \mu_2, \mu_3$ . Without ordering in  $\theta$ , its traceplot shows label-switching in both Gibbs (b) and HMC (c). Slightly relaxed order constraints via CORE allows easy computation and substantially less label-switching (d).

## 6 Sparse Latent Factor Modeling of Brain Networks

We apply CORE to analyze brain networks from the KKI-42 dataset (Landman et al., 2011), which consists of two scans for  $n = 21$  healthy subjects without any history of

neurological disease. For each subject, we take the first scan as the input data, and reserve the second scan for model validation. Data consist of an  $R \times R$  symmetric adjacency matrix  $A_i$ , for  $i = 1, \dots, n$ , with  $R = 68$  the number of brain regions and  $A_{ikl} \in \{0, 1\}$  a 0-1 indicator of a connection between regions  $k$  and  $l$  for individual  $i$ .

Our focus is on characterizing variation among individuals in their brain networks via a latent factor model, with each factor impacting a subset of the brain regions. We assume the elements of  $A_i$  are conditionally independent given latent factors  $v_i = (v_{i1}, \dots, v_{id})'$ , with

$$A_{ikl} \sim \text{Bern}(\pi_{ikl}), \quad \log \left( \frac{\pi_{ikl}}{1 - \pi_{ikl}} \right) = \mu_{kl} + \psi_{ikl}, \quad \psi_{ikl} = \sum_{s=1}^d v_{is} u_{ks} u_{ls}, \quad (17)$$

where  $\mu_{kl}$  characterizes the overall log-odds of an connection in the  $(k, l)$  pair of brain regions, and  $\psi_{ikl}$  is a subject-specific deviation. The latent factor  $v_{is}$  measures how much individual  $i$  expresses brain subnetwork  $s$ , while  $\{u_{k1}, \dots, u_{kd}\}$  are scores measuring impact of brain region  $k$  on the different subnetworks. We let  $\mu_{kl} \sim \text{No}(0, \sigma_\mu^2)$ , with  $\sigma_\mu^2 \sim \text{IG}(2, 1)$ , as a shrinkage prior for the intercept paramters. We similarly let  $v_{is} \sim \text{No}(0, \sigma_s^2)$ , with  $\sigma_s^2 \sim \text{IG}(2, 1)$ , to characterize the population distribution of the  $s$ th latent factor.

In order for the model to be identifiable, which is important for interpretability, the matrix  $U = \{u_{ks}\}$  needs to be restricted. A natural constraint is to assume  $U \in \mathcal{V}(n, d) = \{U : U'U = I_d\}$ , corresponding to the Stiefel manifold, to remove rotation and scaling ambiguity (Hoff, 2016). However, there are limited distributional options available on the Stiefel, and it is not clear how to impose sparsity in  $U$ , so that not all brain regions relate to all latent factors. To solve this problem, we propose to use a Stiefel constraint relaxed Dirichlet-Laplace (DL) shrinkage prior for  $U$ . The DL prior was proposed recently as a computationally convenient and theoretically support prior for incorporating (approximate) sparsity. By multiplying the DL prior by  $\exp(-\lambda^{-1}\|U'U - I\|)$ , with  $\lambda = 10^{-3}$ , we obtain a

prior that generates realizations  $U$  that are very close to orthonormal and sparse.

We compare the resulting model with (i) choosing independent  $\text{No}(0, 1)$  priors for  $u_{ks}$  without constraints; and (ii) choosing such priors with CORE but no DL shrinkage. For each model, we run HMC for 10,000 iterations and discard the first 5,000 iterations as burn-in. For each iteration, we run 300 leap-frog steps. We fixed  $d = 20$  in each case as an upper bound on the number of factors; the shrinkage prior approach can effectively delete factors that are unnecessary for characterizing the data.

As anticipated, the non-CORE models that did not constrain  $U$  failed to converge; one could obtain convergence for identifiable functionals of the parameters, but not directly for the components in the latent factor expansion. The  $\text{No}(0, 1)$  and DL shrinkage CORE models both had good apparent convergence and mixing rates. Figure 5(b) plots the top 6 brain region factors  $U_s = \{u_{1s}, \dots, u_{Rs}\}$  under the normal and shrinkage priors. The shrinkage prior leads to increasing numbers of brain regions with scores close to zero as the factor index increases. In addition, shrinkage improves interpretability of the factors; for example, the second factor has positive scores for brain regions in one hemisphere and negative scores for brain regions in the other.

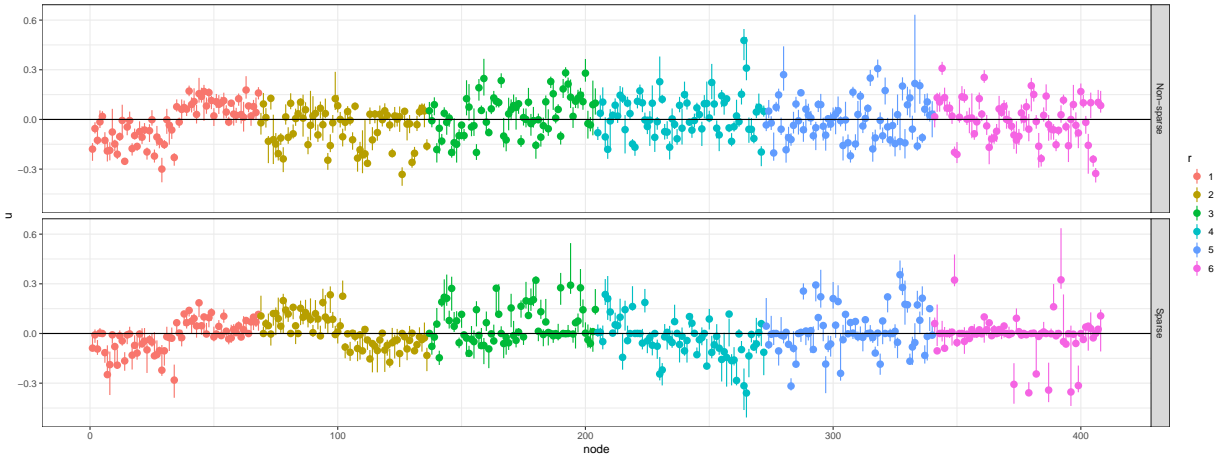


Figure 5: Posterior mean and 95% credible intervals of scores  $U_s = \{u_{1s}, \dots, u_{Rs}\}$  for the  $R = 68$  brain regions, and components  $s = 1, \dots, 6$  (ordered to be decreasing in  $\sigma_s^2$ ).

Model	(i) with shrinkage & near-orthonormality	(ii) with near-orthonormality only	(iii) completely unconstrained
Fitted AUC	97.9%	97.1%	96.9%
Prediction AUC	96.2%	96.2%	93.6%
ESS /1000 Iterations	193.72	188.10	8.15

Table 2: Benchmark of 3 models for 21 brain networks. Models with near-orthonormality show better performance in fitted and prediction AUC, in comparing the estimated probability and the network connectivity. The unconstrained model has low effective sample size (ESS).

We further validate the models by assessing the area under the receiver operating characteristic curve (AUC). We compute the posterior mean of the estimated connectivity probability  $\pi_{ikl}$  for each individual and pair of regions  $(k, l)$ . Thresholding these probabilities produces an adjacency matrix, which we compare with the held-out second scan for each individual. Table 2 lists the benchmark results. The two models under CORE show

much better performance, especially in prediction. Shrinkage does not improve prediction in this case over imposing orthogonality, but nonetheless is useful for interpretability as discussed above.

## References

- Beskos, A., N. Pillai, G. Roberts, J. M. Sanz-Serna, and A. Stuart (2013, 11). Optimal Tuning of the Hybrid Monte Carlo Algorithm. *Bernoulli* 19(5A), 1501–1534.
- Betancourt, M. (2012). Cruising the Simplex: Hamiltonian Monte Carlo and the Dirichlet Distribution. In *AIP Conference Proceedings 31st*, Volume 1443, pp. 157–164. AIP.
- Betancourt, M. (2017). A Conceptual Introduction to Hamiltonian Monte Carlo. *arXiv:1701.02434*.
- Betancourt, M., S. Byrne, and M. Girolami (2014). Optimizing the Integrator Step Size for Hamiltonian Monte Carlo. *arXiv:1411.6669*.
- Boyd, S. and L. Vandenberghe (2004). *Convex Optimization*. Cambridge University Press.
- Byrne, S. and M. Girolami (2013). Geodesic Monte Carlo on Embedded Manifolds. *Scandinavian Journal of Statistics* 40(4), 825–845.
- Diaconis, P., S. Holmes, and M. Shahshahani (2013). Sampling from a Manifold. In *Advances in Modern Statistical Theory and Applications: A Festschrift in honor of Morris L. Eaton*, pp. 102–125. Institute of Mathematical Statistics.
- Evans, L. C. and R. F. Gariepy (2015). *Measure Theory and Fine Properties of Functions*. CRC Press.
- Federer, H. (2014). *Geometric Measure Theory*. Springer.
- Gelfand, A. E., A. F. Smith, and T.-M. Lee (1992). Bayesian Analysis of Constrained Parameter and Truncated Data Problems using Gibbs Sampling. *Journal of the American Statistical Association* 87(418), 523–532.
- Hairer, E., C. Lubich, and G. Wanner (2006). *Geometric Numerical Integration. Structure-Preserving Algorithms for Ordinary Differential Equations*. Springer-Verlag.

- Hoff, P. D. (2009). Simulation of the Matrix Bingham–von Mises–Fisher Distribution, with Applications to Multivariate and Relational Data. *Journal of Computational and Graphical Statistics* 18(2), 438–456.
- Hoff, P. D. (2016). Equivariant and Scale-free Tucker Decomposition Models. *Bayesian Analysis* 11(3), 627–648.
- Hoffman, M. D. and A. Gelman (2014). The No-U-TURN Sampler: Adaptively Setting Path Lengths in Hamiltonian Monte Carlo. *Journal of Machine Learning Research* 15(1), 1593–1623.
- Khatri, C. and K. Mardia (1977). The von Mises-Fisher Matrix Distribution in Orientation Statistics. *Journal of the Royal Statistical Society. Series B (Methodological)*, 95–106.
- Landman, B. A., A. J. Huang, A. Gifford, D. S. Vikram, I. A. L. Lim, J. A. Farrell, J. A. Bogovic, J. Hua, M. Chen, and S. Jarso (2011). Multi-parametric Neuroimaging Reproducibility: a 3-T Resource Study. *Neuroimage* 54(4), 2854–2866.
- Lin, L. and D. B. Dunson (2014). Bayesian Monotone Regression Using Gaussian Process Projection. *Biometrika* 101(2), 303–317.
- Neal, R. M. (2011). MCMC using Hamiltonian Dynamics. *Handbook of Markov Chain Monte Carlo* 2, 113–162.

## Appendix

### A Proofs for Section 3.1

*Proof.* (Lemma 1) Recall, that the distance function  $\|\nu_{\mathcal{D}}(\theta)\|$  is chosen so that  $\|\nu_{\mathcal{D}}(\theta)\|$  is zero for all  $\theta \in \mathcal{D}$ . It follows that for any function  $g(\theta)$

$$\begin{aligned} & \int_{\mathcal{R}} g(\theta) \mathcal{L}(\theta; Y) \pi_{\mathcal{R}}(\theta) \exp(-\|\nu_{\mathcal{D}}(\theta)\|/\lambda) d\mu_{\mathcal{R}}(\theta) \\ &= \int_{\mathcal{R} \setminus \mathcal{D}} g(\theta) \mathcal{L}(\theta; Y) \pi_{\mathcal{R}}(\theta) \exp(-\|\nu_{\mathcal{D}}(\theta)\|/\lambda) d\mu_{\mathcal{R}}(\theta) + \int_{\mathcal{D}} g(\theta) \mathcal{L}(\theta; Y) \pi_{\mathcal{R}}(\theta) d\mu_{\mathcal{R}}(\theta). \end{aligned} \tag{18}$$

For brevity, we let  $f(\theta) = \mathcal{L}(\theta; Y)\pi_{\mathcal{R}}(\theta)$  and use  $df(\theta) = \mathcal{L}(\theta; Y)\pi_{\mathcal{R}}(\theta)d\mu_{\mathcal{R}}(\theta)$  throughout the proof. Then,

$$\begin{aligned} \left| \mathbb{E}[g(\theta)|\theta \in \mathcal{D}] - \mathbb{E}_{\tilde{\pi}_{\lambda}}[g(\theta)] \right| &= \left| \frac{\int_{\mathcal{D}} g(\theta)df(\theta)}{\int_{\mathcal{D}} df(\theta)} - \frac{\int_{\mathcal{R}} g(\theta) \exp(-\|\nu_{\mathcal{D}}(\theta)\|/\lambda)df(\theta)}{\int_{\mathcal{R}} \exp(-\|\nu_{\mathcal{D}}(\theta)\|/\lambda)df(\theta)} \right| \\ &= \left| \frac{\int_{\mathcal{R} \setminus \mathcal{D}} \exp(-\|\nu_{\mathcal{D}}(\theta)\|/\lambda)df(\theta) \int_{\mathcal{D}} g(\theta)df(\theta) - \int_{\mathcal{D}} df(\theta) \int_{\mathcal{R} \setminus \mathcal{D}} g(\theta) \exp(-\|\nu_{\mathcal{D}}(\theta)\|/\lambda)df(\theta)}{\int_{\mathcal{D}} df(\theta) [\int_{\mathcal{D}} df(\theta) + \int_{\mathcal{R} \setminus \mathcal{D}} \exp(-\|\nu_{\mathcal{D}}(\theta)\|/\lambda)df(\theta)]} \right| \end{aligned}$$

where the second equality follows from combining the fractions and making use of (18). We can bound the denominator from below by  $C_{\mathcal{D}}^2 = [\int_{\mathcal{D}} \mathcal{L}(\theta; Y)\pi_{\mathcal{R}}(\theta)d\mu_{\mathcal{R}}(\theta)]^2 > 0$  so that

$$\begin{aligned} &|\mathbb{E}[g(\theta)|\theta \in \mathcal{D}] - \mathbb{E}_{\tilde{\pi}_{\lambda}}[g(\theta)]| \\ &\leq \frac{|\int_{\mathcal{R} \setminus \mathcal{D}} \exp(-\|\nu_{\mathcal{D}}(\theta)\|/\lambda)df(\theta) \int_{\mathcal{D}} g(\theta)df(\theta) - \int_{\mathcal{D}} df(\theta) \int_{\mathcal{R} \setminus \mathcal{D}} g(\theta) \exp(-\|\nu_{\mathcal{D}}(\theta)\|/\lambda)df(\theta)|}{C_{\mathcal{D}}^2} \end{aligned}$$

Add and subtract

$$\int_{\mathcal{R} \setminus \mathcal{D}} \mathcal{L}(\theta; Y)\pi_{\mathcal{R}}(\theta) \exp(-\|\nu_{\mathcal{D}}(\theta)\|/\lambda)df(\theta) \int_{\mathcal{R} \setminus \mathcal{D}} g(\theta) \mathcal{L}(\theta; Y)\pi_{\mathcal{R}}(\theta) \exp(-\|\nu_{\mathcal{D}}(\theta)\|/\lambda)df(\theta)$$

within the numerator, and apply the triangle inequality. Thus,

$$\begin{aligned} &|\mathbb{E}[g(\theta)|\theta \in \mathcal{D}] - \mathbb{E}_{\tilde{\pi}_{\lambda}}[g(\theta)]| \\ &\leq \frac{\left| \int_{\mathcal{R} \setminus \mathcal{D}} \exp(-\|\nu_{\mathcal{D}}(\theta)\|/\lambda)df(\theta) \left| \int_{\mathcal{D}} g(\theta)df(\theta) - \int_{\mathcal{R} \setminus \mathcal{D}} g(\theta) \exp(-\|\nu_{\mathcal{D}}(\theta)\|/\lambda)df(\theta) \right| \right|}{C_{\mathcal{D}}^2} \\ &\quad + \frac{\left| \int_{\mathcal{R} \setminus \mathcal{D}} g(\theta) \exp(-\|\nu_{\mathcal{D}}(\theta)\|/\lambda)df(\theta) \right| \left| \int_{\mathcal{D}} df(\theta) - \int_{\mathcal{R} \setminus \mathcal{D}} \exp(-\|\nu_{\mathcal{D}}(\theta)\|/\lambda)df(\theta) \right|}{C_{\mathcal{D}}^2} \end{aligned}$$

Since  $g \in \mathbb{L}^1(\mathcal{R}, \mathcal{L}(\theta; Y)\pi_{\mathcal{R}}(\theta)d\mu_{\mathcal{R}})$ , we can bound the numerators. First,

$$\begin{aligned} &\left| \int_{\mathcal{R} \setminus \mathcal{D}} \exp(-\|\nu_{\mathcal{D}}(\theta)\|/\lambda)df(\theta) \right| \left| \int_{\mathcal{D}} g(\theta)df(\theta) - \int_{\mathcal{R} \setminus \mathcal{D}} g(\theta) \exp(-\|\nu_{\mathcal{D}}(\theta)\|/\lambda)df(\theta) \right| \\ &\leq \int_{\mathcal{R} \setminus \mathcal{D}} \exp(-\|\nu_{\mathcal{D}}(\theta)\|/\lambda)df(\theta) \int_{\mathcal{R}} |g(\theta)|df(\theta) = C_{\mathcal{R}} \mathbb{E}|g(\theta)| \int_{\mathcal{R} \setminus \mathcal{D}} \exp(-\|\nu_{\mathcal{D}}(\theta)\|/\lambda)df(\theta). \end{aligned}$$

Here,  $C_{\mathcal{R}} = \int_{\mathcal{R}} df(\theta)$  is the normalizing constant of  $\mathcal{L}(\theta; Y)\pi_{\mathcal{R}}(\theta)$ . Secondly,

$$\begin{aligned} & \left| \int_{\mathcal{R} \setminus \mathcal{D}} g(\theta) \exp(-\|\nu_{\mathcal{D}}(\theta)\|/\lambda) df(\theta) \right| \left| \int_{\mathcal{D}} df(\theta) - \int_{\mathcal{R} \setminus \mathcal{D}} \exp(-\|\nu_{\mathcal{D}}(\theta)\|/\lambda) df(\theta) \right| \\ &= C_{\mathcal{R}} \int_{\mathcal{R} \setminus \mathcal{D}} |g(\theta)| \exp(-\|\nu_{\mathcal{D}}(\theta)\|/\lambda) df(\theta). \end{aligned}$$

Thus, we have the bounds specified by the theorem,

$$|\mathbb{E}[g(\theta)|\theta \in \mathcal{D}] - \mathbb{E}_{\tilde{\pi}_{\lambda}}[g(\theta)]| = \frac{C_{\mathcal{R}} \int_{\mathcal{R} \setminus \mathcal{D}} (\mathbb{E}|g(\theta)| + |g(\theta)|) \exp(-\|\nu_{\mathcal{D}}(\theta)\|/\lambda) df(\theta)}{C_{\mathcal{D}}^2}.$$

By assumption,  $g \in \mathbb{L}^1(\mathcal{R}, \mathcal{L}(\theta; Y)\pi_{\mathcal{R}}(\theta)d\mu_{\mathcal{R}})$  and  $\|\nu_{\mathcal{D}}(\theta)\| > 0$  for  $\mu_{\mathcal{R}}$  a.e.  $\theta \in \mathcal{R} \setminus \mathcal{D}$ . It follows that  $(\mathbb{E}|g(\theta)| + |g(\theta)|)f(\theta)$  is a dominating function of  $(\mathbb{E}|g(\theta)| + |g(\theta)|)f(\theta) \exp(-\|\nu_{\mathcal{D}}(\theta)\|/\lambda)$  which converges to zero for  $\mu_{\mathcal{R}}$ -a.e.  $\theta \in \mathcal{R} \setminus \mathcal{D}$  as  $\lambda \rightarrow 0^+$ . Thus,  $|\mathbb{E}[g(\theta)|\theta \in \mathcal{D}] - \mathbb{E}_{\tilde{\pi}_{\lambda}}[g(\theta)]| \rightarrow 0$  as  $\lambda \rightarrow 0^+$ .  $\square$

*Proof.* (Theorem 1) We begin with the bound from Lemma 1.

$$|\mathbb{E}[g(\theta)|\theta \in \mathcal{D}] - \mathbb{E}_{\tilde{\pi}_{\lambda}}[g(\theta)]| \leq \frac{C_{\mathcal{R}} \int_{\mathcal{R} \setminus \mathcal{D}} (\mathbb{E}|g(\theta)| + |g(\theta)|) \mathcal{L}(\theta; Y)\pi_{\mathcal{R}}(\theta) \exp(-\|\nu_{\mathcal{D}}(\theta)\|/\lambda) d\mu_{\mathcal{R}}(\theta)}{C_{\mathcal{D}}^2}.$$

Applying the Cauchy-Schwartz inequality to the numerator,

$$\begin{aligned} & C_{\mathcal{R}} \int_{\mathcal{R} \setminus \mathcal{D}} (\mathbb{E}|g(\theta)| + |g(\theta)|) \exp(-\|\nu_{\mathcal{D}}(\theta)\|/\lambda) df(\theta) \\ & \leq C_{\mathcal{R}} \left( \int_{\mathcal{R} \setminus \mathcal{D}} (\mathbb{E}|g(\theta)| + |g(\theta)|)^2 df(\theta) \right)^{1/2} \left( \int_{\mathcal{R} \setminus \mathcal{D}} \exp(-2\|\nu_{\mathcal{D}}(\theta)\|/\lambda) df(\theta) \right)^{1/2} \end{aligned}$$

By assumption,  $g \in \mathbb{L}^2(\mathcal{R}, \mathcal{L}(\theta; Y)\pi_{\mathcal{R}}(\theta)d\mu_{\mathcal{R}})$ . Thus,

$$C_{\mathcal{R}} \int_{\mathcal{R} \setminus \mathcal{D}} (\mathbb{E}|g(\theta)| + |g(\theta)|) \exp(-\|\nu_{\mathcal{D}}(\theta)\|/\lambda) df(\theta) \leq C_g \left( \int_{\mathcal{R} \setminus \mathcal{D}} \exp(-2\|\nu_{\mathcal{D}}(\theta)\|/\lambda) df(\theta) \right)^{1/2}$$

where  $C_g = \left(3C_{\mathcal{R}}^2(\mathbb{E}|g|)^2 + C_{\mathcal{R}}\mathbb{E}[|g|^2]\right)^{1/2}$ . We separate the integral  $\int_{\mathcal{R} \setminus \mathcal{D}} \exp(-2\|\nu_{\mathcal{D}}(\theta)\|/\lambda) df(\theta)$  over the sets  $\Lambda = \{\theta : 0 < \|\nu_{\mathcal{D}}(\theta)\| < -\lambda \log \lambda\}$  and  $\Lambda^c = \{\theta : \|\nu_{\mathcal{D}}(\theta)\| > -\lambda \log \lambda\}$ .

$$\begin{aligned} \int_{\mathcal{R} \setminus \mathcal{D}} \exp(-2\|\nu_{\mathcal{D}}(\theta)\|/\lambda) df(\theta) &= \int_{\Lambda^c} \exp(-2\|\nu_{\mathcal{D}}(\theta)\|/\lambda) df(\theta) + \int_{\Lambda} \exp(-2\|\nu_{\mathcal{D}}(\theta)\|/\lambda) df(\theta) \\ &\leq \lambda^2 \int_{\Lambda^c} df(\theta) + \int_{\Lambda} \exp(-2\|\nu_{\mathcal{D}}(\theta)\|/\lambda) df(\theta) = C_{\mathcal{R}} \lambda^2 + \int_{\Lambda} \exp(-2\|\nu_{\mathcal{D}}(\theta)\|/\lambda) df(\theta) \end{aligned}$$

From the requirements of Theorem 1, we now let  $\|\nu_{\mathcal{D}}(\theta)\| = \inf_{x \in \mathcal{D}} \|\theta - x\|_2$  and assume that  $\mathcal{D}$  has a piecewise smooth boundary. In this case, the set  $\Lambda = \{\theta : 0 < \|\nu_{\mathcal{D}}(\theta)\| < -\lambda \log \lambda\}$  forms a ‘shell’ of thickness  $-\lambda \log \lambda$  which encases  $\mathcal{D}$ .

In this case,  $J(\nu_{\mathcal{D}}(\theta)) = 2$ . By the co-area formula (Diaconis et al. (2013); Federer (2014))

$$\int_{\Lambda} \exp(-2\|\nu_{\mathcal{D}}(\theta)\|/\lambda) df(\theta) = \int_0^{-\lambda \log \lambda} e^{-\frac{x}{\lambda}} \left( \int_{\nu_{\mathcal{D}}^{-1}(x)} \frac{1}{2} f(\theta) d\bar{\mathcal{H}}^{r-1}(\theta) \right) dx$$

Again, we may take  $\lambda$  sufficiently small so that  $f(\theta) = \mathcal{L}(\theta; Y)\pi_{\mathcal{R}}(\theta)$  is continuous on  $\Lambda$ . As such, the function  $\int_{\nu_{\mathcal{D}}^{-1}(x)} \frac{1}{2} f(\theta) d\bar{\mathcal{H}}^{r-1}(\theta)$  is a continuous map from the closed interval  $[0, -\lambda \log \lambda]$  to  $\mathbb{R}$ ; hence, it is bounded. As a result,

$$\begin{aligned} \int_{\Lambda} \exp(-2\|\nu_{\mathcal{D}}(\theta)\|/\lambda) df(\theta) &\leq \sup_{x \in [0, -\lambda \log \lambda]} \left( \int_{\nu_{\mathcal{D}}^{-1}(x)} \frac{1}{2} \mathcal{L}(\theta; Y)\pi_{\mathcal{R}}(\theta) d\bar{\mathcal{H}}^{r-1}(\theta) \right) \int_0^{-\lambda \log \lambda} e^{-\frac{x}{\lambda}} dx \\ &= \sup_{x \in [0, -\lambda \log \lambda]} \left( \int_{\nu_{\mathcal{D}}^{-1}(x)} \frac{1}{2} \mathcal{L}(\theta; Y)\pi_{\mathcal{R}}(\theta) d\bar{\mathcal{H}}^{r-1}(\theta) \right) (\lambda - \lambda^2) = O(\lambda) \end{aligned}$$

Thus, we may conclude that

$$\begin{aligned} |\mathbb{E}[g(\theta) | \theta \in \mathcal{D}] - \mathbb{E}_{\tilde{\pi}_{\lambda}}[g(\theta)]| &\leq \frac{C_g}{C_{\mathcal{D}}^2} \left( C_{\mathcal{R}} \lambda^2 + \sup_{x \in [0, -\lambda \log \lambda]} \left( \int_{\nu_{\mathcal{D}}^{-1}(x)} \frac{1}{2} f(\theta) d\bar{\mathcal{H}}^{r-1}(\theta) \right) (\lambda - \lambda^2) \right)^{1/2} \\ &= \frac{C_g}{C_{\mathcal{D}}^2} \sup_{x \in [0, -\lambda \log \lambda]} \left( \int_{\nu_{\mathcal{D}}^{-1}(x)} \frac{1}{2} f(\theta) d\bar{\mathcal{H}}^{r-1}(\theta) \right) \sqrt{\lambda} + o(\sqrt{\lambda}) \end{aligned}$$

Since  $\sup_{x \in [0, -\lambda \log \lambda]} \left( \int_{\nu_{\mathcal{D}}^{-1}(x)} \frac{1}{2} f(\theta) d\bar{\mathcal{H}}^{r-1}(\theta) \right)$  is a decreasing function in  $\lambda$ , it follows that

$$|\mathbb{E}[g(\theta) | \theta \in \mathcal{D}] - \mathbb{E}_{\tilde{\pi}_{\lambda}}[g(\theta)]| = O(\sqrt{\lambda}) \text{ as } \lambda \rightarrow 0^+.$$

□

## B Proofs from Section 3.2

*Proof.* (Theorem 4) Again for brevity, we continue with the notation  $f(\theta) = \mathcal{L}(\theta; Y)\pi_{\mathcal{R}}(\theta)$  and  $df(\theta) = \mathcal{L}(\theta; Y)\pi_{\mathcal{R}}(\theta)d\mu_{\mathcal{R}}(\theta)$ . Recall that we have two densities. The first is the fully constrained density for  $\theta \in \mathcal{D}$ ,

$$\pi_{\mathcal{D}}(\theta) = \frac{1}{m_0} \frac{\mathcal{L}(\theta; Y)\pi_{\mathcal{R}}(\theta)}{J(\nu_{\mathcal{D}}(\theta))} \mathbb{1}_{\mathcal{D}}(\theta) = \frac{1}{m_0} \frac{f(\theta)}{J(\nu_{\mathcal{D}}(\theta))} \mathbb{1}_{\mathcal{D}}(\theta)$$

where the normalizing constant  $m_0 = \int_{\mathcal{R}} \frac{f(\theta)}{J(\nu_{\mathcal{D}}(\theta))} \mathbb{1}_{\mathcal{D}}(\theta) d\bar{\mathcal{H}}^{r-s}(\theta)$  is calculated with respect to the normalized Hausdorff measure. Secondly, we have the relaxed distribution

$$\tilde{\pi}_{\mathcal{D}}(\theta) = \frac{1}{m_{\lambda}} \mathcal{L}(\theta; Y)\pi_{\mathcal{R}}(\theta) \exp\left(-\frac{\|\nu_{\mathcal{D}}(\theta)\|_1}{\lambda}\right) = \frac{1}{m_{\lambda}} f(\theta) \exp\left(-\frac{\|\nu_{\mathcal{D}}(\theta)\|_1}{\lambda}\right)$$

where the normalizing constant  $m_{\lambda} = \int_{\mathcal{R}} f(\theta) \exp\left(-\frac{\|\nu_{\mathcal{D}}(\theta)\|_1}{\lambda}\right) d\mu_{\mathcal{R}}(\theta)$  is calculated with respect to Lebesgue measure on  $\mathcal{R}$ .

For a given function,  $g : \mathcal{R} \rightarrow \mathbb{R}$ , we can define the expectation of  $g(\theta)$  under the sharp and relaxed posteriors, denoted by  $\mathbb{E}$  and  $\mathbb{E}_{\tilde{\Pi}}$  respectively, as

$$\begin{aligned} \mathbb{E}[g(\theta) | \theta \in \mathcal{D}] &= \int_{\mathcal{R}} \frac{g(\theta)}{m_0} \frac{f(\theta)}{J(\nu_{\mathcal{D}}(\theta))} \mathbb{1}_{\mathcal{D}}(\theta) d\bar{\mathcal{H}}^{r-s}(\theta) \\ \mathbb{E}_{\tilde{\Pi}}[g(\theta)] &= \int_{\mathbb{R}^s} \frac{\exp\left(-\frac{\|x\|_1}{\lambda}\right)}{m_{\lambda}} \int_{\nu_{\mathcal{D}}^{-1}(x)} g(\theta) \frac{f(\theta)}{J(\nu_{\mathcal{D}}(\theta))} d\bar{\mathcal{H}}^{r-s}(\theta) d\mu_{\mathbb{R}^s}(x). \end{aligned}$$

The second equality follows from the co-area formula applied to (14). By construction,  $m(x) = m^{r-s}(x) = \int_{\nu_{\mathcal{D}}^{-1}(x)} \frac{f(\theta)}{J(\nu_{\mathcal{D}}(\theta))} d\bar{\mathcal{H}}^{r-s}(\theta) > 0$  for  $\mu_{\mathbb{R}^s}$ -a.e.  $x \in \text{Range}(\nu_{\mathcal{D}})$ . Notably,  $m_0 = m(0) > 0$ . By Theorem 3,

$$\mathbb{E}[g(\theta) | \nu_{\mathcal{D}}(\theta) = x] = \frac{1}{m(x)} \int_{\nu_{\mathcal{D}}^{-1}(x)} g(\theta) \frac{f(\theta)}{J(\nu_{\mathcal{D}}(\theta))} d\bar{\mathcal{H}}^{r-s}(\theta) = \frac{G(x)}{m(x)}. \quad (19)$$

As such, we may express  $\mathbb{E}_{\tilde{\Pi}}[g(\theta)]$  as

$$\mathbb{E}_{\tilde{\Pi}}[g(\theta)] = \int_{\mathbb{R}^s} \frac{m(x)}{m_{\lambda}} \exp\left(-\frac{\|x\|_1}{\lambda}\right) \mathbb{E}[g(\theta) | \nu_{\mathcal{D}}(\theta) = x] d\mu_{\mathbb{R}^s}(x). \quad (20)$$

Let us first consider the small  $\lambda$  behavior of  $m_\lambda$ . We begin by re-expressing  $m_\lambda$  in terms of  $m(x)$  through the co-area formula.

$$m_\lambda = \int_{\mathbb{R}^s} \exp\left(-\frac{\|x\|_1}{\lambda}\right) \int_{\nu_{\mathcal{D}}^{-1}(x)} \frac{f(\theta)}{J(\nu_{\mathcal{D}}(\theta))} d\bar{\mathcal{H}}^{r-s}(\theta) d\mu_{\mathbb{R}^s}(x) = \int_{\mathbb{R}^s} m(x) \exp\left(-\frac{\|x\|_1}{\lambda}\right) d\mu_{\mathbb{R}^s}(x)$$

Split the above integral into two regions:  $\Lambda = \{x \in \mathbb{R}^s : 0 \leq \|x\|_1 \leq \lambda |\log(\lambda^{s+1})|\}$  and  $\Lambda^c$ . Note that over  $\Lambda^c$ ,  $\exp(-\|x\|_1/\lambda) < \lambda^{s+1}$ .

$$\begin{aligned} m_\lambda &= \int_{\Lambda^c} m(x) \exp\left(-\frac{\|x\|_1}{\lambda}\right) d\mu_{\mathbb{R}^s}(x) + \int_{\Lambda} m(x) \exp\left(-\frac{\|x\|_1}{\lambda}\right) d\mu_{\mathbb{R}^s}(x) \\ &= O\left(\lambda^{s+1}\right) + \int_{\Lambda} m(x) \left[1 + O\left(\frac{1}{\lambda} \exp\left(-\frac{\|x\|_1}{\lambda}\right)\right)\right] d\mu_{\mathbb{R}^s}(x) \\ &= O\left(\lambda^{s+1}\right) + \int_{\Lambda} m(x) \left[1 + O(\lambda^s)\right] d\mu_{\mathbb{R}^s}(x) \end{aligned}$$

Since  $m(x)$  is continuous on an open neighborhood containing the origin, we may choose  $\lambda$  small enough so that  $m(x)$  is uniformly continuous on  $\Lambda$ . Then,

$$m_\lambda = O\left(\lambda^{s+1}\right) + \int_{\Lambda} [m(0) + o(1)][1 + O(\lambda^s)] d\mu_{\mathbb{R}^s}(x) = m(0) \frac{|2(s+1)\lambda \log \lambda|^s}{\Gamma(s+1)} + o(|\lambda \log \lambda|^s)$$

at leading order as  $\lambda \rightarrow 0^+$ . Here,  $|2(s+1)\lambda \log \lambda|^s/\Gamma(s+1)$  is the Lebesgue measure of  $\Lambda$ .

We now turn to the small  $\lambda$  behavior of  $\mathbb{E}_{\tilde{\Pi}}[g(\theta)]$ . Similar to the study of  $m_\lambda$ , separate  $\mathbb{E}_{\tilde{\Pi}}[g(\theta)]$  into integrals over  $\Lambda$  and  $\Lambda^c$ . Again, we may choose  $\lambda$  sufficient small so that both  $m(x)$  and  $G(x) = \int_{\nu_{\mathcal{D}}^{(-1)}(x)} g(\theta) \frac{f(\theta)}{J(\nu_{\mathcal{D}}(\theta))} d\bar{\mathcal{H}}^{r-s}(\theta)$  are continuous on  $\Lambda$  and hence uniformly continuous at  $x = 0$ . Additionally, the positivity of  $m(0)$  implies that  $\mathbb{E}[g(\theta)|\nu_{\mathcal{D}}(\theta) = x]$  is also uniformly continuous at  $x = 0$ . Therefore,

$$\begin{aligned} \mathbb{E}_{\tilde{\Pi}}[g(\theta)] &= \int_{\Lambda^c} \frac{\exp\left(-\frac{\|x\|_1}{\lambda}\right)}{m_\lambda} m(x) \mathbb{E}[g(\theta)|\nu_{\mathcal{D}}(\theta) = x] d\mu_{\mathbb{R}^s}(x) \\ &\quad + \int_{\Lambda} \frac{1 + o(1)}{m(0) \frac{|2(s+1)\lambda \log \lambda|^s}{\Gamma(s+1)} + o(\lambda |\log \lambda|^s)} [m(0) + o(1)] [\mathbb{E}[g(\theta)|\nu_{\mathcal{D}}(\theta) = 0] + o(1)] d\mu_{\mathbb{R}^s}(x) \\ &= O\left(\frac{\lambda^{s+1}}{m_\lambda}\right) + \mathbb{E}[g(\theta)|\nu_{\mathcal{D}}(\theta) = 0] + o(1) = \mathbb{E}[g(\theta)|\theta \in \mathcal{D}] + O\left(\frac{\lambda}{|\log \lambda|^s}\right) + o(1). \end{aligned}$$

And we may conclude that  $|\mathbb{E}[g|\theta \in \mathcal{D}] - \mathbb{E}_{\tilde{\Pi}}[g]| \rightarrow 0$  as  $\lambda \rightarrow 0^+$ .

The proof of the corollary follows by changing the  $o(1)$  correction within the integrals over  $\Lambda$  to  $O(\lambda|\log \lambda^{s+1}|)$  corrections. As a result, the leading order error is then  $O(\lambda|\log \lambda|^{-s})$  as  $\lambda \rightarrow 0^+$ .  $\square$

## C Supplementary Materials

### C.1 Support Expansion Near a Curved Torus

Let  $\mathcal{R} = \mathbb{R}^3$  and consider a curved torus

$$\mathcal{D} = \{\theta : (\theta_1, \theta_2, \theta_3) = ((1+0.5 \cos \alpha_1) \cos \alpha_2, (1+0.5 \cos \alpha_1) \sin \alpha_2, 0.5 \sin \alpha_1), (\alpha_1, \alpha_2) \in [0, 2\pi]^2\},$$

which has intrinsic dimension two and zero 3-dimensional Lebesgue measure,  $\mu_{\mathcal{R}}(\mathcal{D}) = 0$ . Diaconis et al. (2013) proposed an algorithm for sampling from a uniform density with respect to Hausdorff measure over this compact manifold.

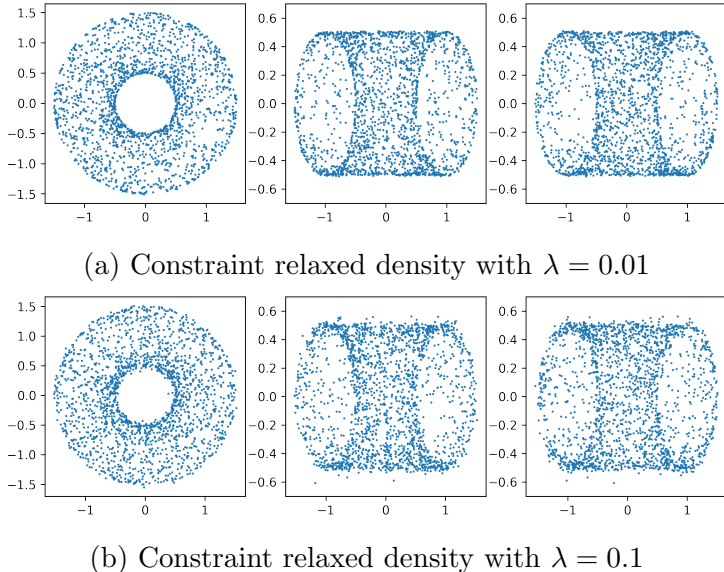


Figure 6: Samples from constraint relaxed based on a uniform density on a torus. As  $\lambda$  increases, more points are generated outside of the torus.

The torus  $\mathcal{D}$  can be defined implicitly as the solution set to the equation

$$\nu_{\mathcal{D}}(\theta) = \left(1 - \sqrt{\theta_1^2 + \theta_2^2}\right)^2 + \theta_3^2 - \frac{1}{4} = 0.$$

Using this, we can replace the uniform density over the torus with the relaxed density

$$\begin{aligned}\tilde{\pi}_\lambda(\theta) &\propto J(\nu_{\mathcal{D}}(\theta)) \exp(-\lambda^{-1}\|\nu_{\mathcal{D}}(\theta)\|) \\ &= 2\sqrt{(1 - \sqrt{\theta_1^2 + \theta_2^2})^2 + \theta_3^2} \exp\left\{-\lambda^{-1}\left|\left(1 - \sqrt{\theta_1^2 + \theta_2^2}\right)^2 + \theta_3^2 - \frac{1}{4}\right|\right\}\end{aligned}\quad (21)$$

which is defined with respect to 3-dimensional Lebesgue measure. Here we initially multiplied the relaxed distribution by the Jacobian so that we attain uniform sampling on the torus under the sharp constraint,

$$\pi_{\mathcal{D}}(\theta) \propto \frac{J(\nu_{\mathcal{D}}(\theta)) \mathbb{1}_{\mathcal{D}}(\theta)}{J(\nu_{\mathcal{D}}(\theta))} = \mathbb{1}_{\mathcal{D}}(\theta).$$

Figure 6 plots random samples from relaxed distribution to uniform densities over the torus for two different values of  $\lambda$ , corresponding to different degrees of relaxation.

## C.2 Computing Efficiency in CORE-HMC

It is interesting to study the effect of relaxation on computing efficiency of HMC. In understanding computational efficiency of HMC, it is useful to consider the number of leapfrog steps to be a function of  $\epsilon$  and set  $L = \lfloor \tau/\epsilon \rfloor$  for a fixed integration time  $\tau > 0$ . In this case, the mixing rate is determined by  $\tau$  in the limit  $\epsilon \rightarrow 0$  (Betancourt, 2017). While a smaller stepsize  $\epsilon$  leads to a more accurate numerical approximation of Hamiltonian dynamics and hence a higher acceptance rate, it takes a larger number of leapfrog steps and gradient evaluations to achieve good mixing. For computational efficiency, the stepsize  $\epsilon$  should be chosen only as small as needed to achieve a reasonable acceptance rate (Beskos et al., 2013; Betancourt et al., 2014). A critical factor in determining a reasonable stepsize is the *stability limit* of the leapfrog integrator (Neal, 2011). When  $\epsilon$  exceeds this limit, the approximation becomes unstable and the acceptance rate drops dramatically. Below the stability limit, the acceptance rate  $a(\epsilon)$  of HMC increases to 1 quite rapidly as  $\epsilon \rightarrow 0$  and satisfies  $a(\epsilon) = 1 - \mathcal{O}(\epsilon^4)$  (Beskos et al., 2013).

For simplicity, the following discussions assume the mass matrix  $M$  is the identity, and  $\mathcal{D} = \cap_{j=1}^s \{\theta : \nu_j(\theta) = 0\}$ . We denote  $\mathcal{D}_j = \{\theta : \nu_j(\theta) = 0\}$  and consider a directional relaxation, which lets  $\exp(-\sum_j \|\nu_j(\theta^*)\| \lambda_j^{-1})$ . Typically, the stability limit of the leapfrog integrator is closely related to the largest eigenvalue  $\xi_1(\theta)$  of the Hessian matrix  $\mathbf{H}_U(\theta)$  of  $U(\theta) = -\log \pi(\theta)$ . Linear stability analysis and empirical evidence suggest that, for stable approximation of Hamiltonian dynamics by the leapfrog integrator in  $\mathbb{R}^p$ , the condition

$\epsilon < 2\xi_1(\theta)^{-1/2}$  must hold on most regions of the parameter space (Hairer et al., 2006). Under the CORE framework, the Hessian is given by

$$\mathbf{H}_U(\theta) = -\mathbf{H}_{\log(\mathcal{L}(\theta; y)\pi_{\mathcal{R}}(\theta))}(\theta) + \sum_j \lambda_j^{-1} \mathbf{H} \|\nu_j(\theta)\| \mathbb{1}_{\theta \notin \mathcal{D}_j}. \quad (22)$$

For  $\theta \notin \mathcal{D}_j$ , as we make relaxations tighter i.e.  $\lambda_j \rightarrow 0$ , the second term dominates the eigenvalue in the first term and the largest eigenvalue effectively becomes proportional to  $\min_{j: \theta \notin \mathcal{D}_j} \lambda_j^{-1}$ . In other words, if we think of the Hessian as representing local covariance structure in the target distribution, then the effect of constraints on the stability limit becomes significant roughly speaking when  $\min_j \lambda_j^{-1}$  is chosen smaller than the variance of the distribution along  $\mathcal{D}$ .

The above discussion shows that a choice of extremely small  $\lambda_j$  — corresponding to very tight constraints — could create a computational bottleneck for HMC. Additionally, very tight constraints make it difficult for the no-U-turn criterion of Hoffman and Gelman (2014) to appropriately calibrate the number of leapfrog steps because the U-turn condition may be met too early to adequately explore the parameter space. For this reason, it is in general best not to make constraints tighter than necessary. On the other hand, when the leapfrog integrator requires a stepsize  $\epsilon \ll \min_j \lambda_j^{-1/2}$  for an accurate approximation, one can safely make the constraint tighter as desired without affecting computational efficiency of HMC.

In our experience, a small number of experiments with different values of  $\lambda$ 's were sufficient to find out when the constraint starts to become a bottleneck. Also, HMC usually achieved satisfactory sampling efficiency under reasonably tight constraints. We now use a problem of sampling from the von Mises–Fisher distribution to illustrate how a choice of  $\lambda$  affects sampling efficiency.

We test  $\lambda = 10^{-3}, 10^{-4}$  and  $10^{-5}$  for CORE-HMC. Table 3 shows the effective sample size per 1000 iterations, the effective ‘violation’  $|v(\theta)| = |\theta_1^2 + \theta_2^2 - 1|$  and the  $\left| \mathbb{E}_{\Pi}[\sum_j \theta_j] - \mathbb{E}_{\tilde{\Pi}}[\sum_j \theta_j] \right|$  as the measure of relaxation. As the expectation is numerically computed, to provide a baseline, we also compare two independent samples from the same exact distribution. The expectation difference based on  $\lambda = 10^{-5}$  is indistinguishable from this low difference, while the other  $\lambda$  have slightly larger expectation difference but more effective samples.

	HMC based on CORE			Exact
	$\lambda = 10^{-3}$	$\lambda = 10^{-4}$	$\lambda = 10^{-5}$	
$ \mathbb{E}_{\Pi}[\sum_j \theta_j] - \mathbb{E}_{\tilde{\Pi}}[\sum_j \theta_j] $	0.025 (0.014, 0.065)	0.016 (0.012, 0.019)	0.008 (0.006, 0.015)	0.009 (0.007, 0.015)
$ \nu_{\mathcal{D}}(\theta) $	$9 \times 10^{-4}$ ( $2.6 \times 10^{-5}, 3.3 \times 10^{-3}$ )	$9 \times 10^{-5}$ ( $2.0 \times 10^{-6}, 3.4 \times 10^{-4}$ )	$9 \times 10^{-6}$ ( $2.7 \times 10^{-7}, 3.5 \times 10^{-5}$ )	0
ESS /1000 Iterations	751.48	260.54	57.10	788.30

Table 3: Benchmark of constraint relaxation methods on sampling von–Mises Fisher distribution on a unit circle. For each CORE, average expectation difference (with 95% credible interval, out of 10 repeated experiments) is computed, and numeric difference is shown under column ‘exact’ as comparing two independent copies from the exact distribution. Effective sample size shows CORE with relatively large  $\lambda$  have high computing efficiency.